T Cell Antigen Receptor Recognition of Antigen-Presenting Molecules

Jamie Rossjohn,[1,2,3] Stephanie Gras,[1,2] John J. Miles,[3,4] Stephen J. Turner,[5] Dale I. Godfrey,[5,6] and James McCluskey[5]

[1]Department of Biochemistry and Molecular Biology, School of Biomedical Sciences, Monash University, Clayton, Victoria 3800, Australia; email: Jamie.rossjohn@monash.edu, Stephanie.Gras@monash.edu

[2]Australian Research Council Centre of Excellence for Advanced Molecular Imaging, Monash University, Clayton, Victoria 3800, Australia

[3]Institute of Infection and Immunity, Cardiff University, School of Medicine, Heath Park, Cardiff CF14 4XN, United Kingdom

[4]QIMR Berghofer Medical Research Institute and QIMR Berghofer Center for Immunotherapy and Vaccine Development, Brisbane, Queensland 4006, Australia; email: John.Miles@qimr.edu.au

[5]Department of Microbiology and Immunology, Peter Doherty Institute for Infection and Immunity, University of Melbourne, Parkville, Victoria 3010, Australia; email: jamesm1@unimelb.edu.au, sjturn@unimelb.edu.au, godfrey@unimelb.edu.au

[6]Australian Research Council Centre of Excellence for Advanced Molecular Imaging, University of Melbourne, Parkville, Victoria 3010, Australia

Annu. Rev. Immunol. 2015. 33:169–200

First published online as a Review in Advance on December 10, 2014

The *Annual Review of Immunology* is online at immunol.annualreviews.org

This article's doi: 10.1146/annurev-immunol-032414-112334

Keywords

major histocompatibility complex, CD1, MR1, T cell antigen receptor

Abstract

The *Major Histocompatibility Complex* (MHC) locus encodes classical MHC class I and MHC class II molecules and nonclassical MHC-I molecules. The architecture of these molecules is ideally suited to capture and present an array of peptide antigens (Ags). In addition, the CD1 family members and MR1 are MHC class I–like molecules that bind lipid-based Ags and vitamin B precursors, respectively. These Ag-bound molecules are subsequently recognized by T cell antigen receptors (TCRs) expressed on the surface of T lymphocytes. Structural and associated functional studies have been highly informative in providing insight into these interactions, which are crucial to immunity, and how they can lead to aberrant T cell reactivity. Investigators have determined over thirty unique TCR-peptide-MHC-I complex structures and twenty unique TCR-peptide-MHC-II complex structures. These investigations have shown a broad consensus in docking geometry and

provided insight into MHC restriction. Structural studies on TCR-mediated recognition of lipid and metabolite Ags have been mostly confined to TCRs from innate-like natural killer T cells and mucosal-associated invariant T cells, respectively. These studies revealed clear differences between TCR-lipid-CD1, TCR-metabolite-MR1, and TCR-peptide-MHC recognition. Accordingly, TCRs show remarkable structural and biological versatility in engaging different classes of Ag that are presented by polymorphic and monomorphic Ag-presenting molecules of the immune system.

INTRODUCTION

The central interaction in cell-mediated adaptive immunity is between the αβ T cell antigen receptor (αβTCR) and an antigen-presenting molecule loaded with a given antigen (Ag). The αβTCR corecognizes the Ag-Ag-presenting molecule complex, and given the inherent diversity within this system, many potential αβTCR recognition events control T cell immunity. Upon productive αβTCR engagement, the αβTCR transmits signals to the CD3 complex, which subsequently triggers intracellular signaling cascades that lead to effective immunity. The parameters defining productive engagement and αβTCR-CD3 signal transmission are a keenly investigated area (1). The αβTCR recognition event is central to protective immunity against pathogens but also underpins aberrant T cell reactivity (2, 3). Although many studies have focused on the interaction between αβTCRs with peptides (p) presented by the polymorphic members of the major histocompatibility complex (MHC) [human leukocyte antigens (HLA) in humans] (4), it is clear that αβTCRs can recognize other Ags presented by distinct Ag-presenting molecules. Namely, specific αβTCRs bind to lipid-based Ags presented by members of the CD1 family (5). Further, particular αβTCRs bind precursors of vitamin B metabolites that are presented by the MHC class I–related molecule MR1 (6). Moreover, a different family of TCRs consisting of γ- and δ-chain heterodimers (γδTCRs) can recognize MHC-like molecules (7). Thus, investigating the structural basis of TCR recognition events provides key and detailed insight into the ensuing T cell biology that underpins health and disease. Stemming from the seminal finds of TCR recognition (8, 9), the field of structural T cell immunology has progressed substantially (10). Structurally focused investigations have yielded a greater understanding of MHC restriction (11–13), T cell autoimmunity, T cell cross-reactivity/alloreactivity (3, 14), and innate-like T cell recognition of lipid and metabolite Ags (6, 15). Here we review TCR recognition of Ag-presenting molecules.

Structure of Ag-Presenting Molecules

To understand how TCRs can recognize Ags, it is first necessary to determine the structures of these Ag-presenting molecules; this topic was comprehensively reviewed recently (16). The classical MHC molecules are subdivided into MHC class I (MHC-I) and MHC class II (MHC-II), both of which are high polymorphic. The classical MHC-I genes comprise three classes in humans (HLA-A, HLA-B, and HLA-C) and mice (H2-K, H2-D, and H2-L). The MHC-II genes comprise three classes in humans (HLA-DR, HLA-DQ, and HLA-DP) and two classes in mice (H-2A and H-2E). In addition, there are nonclassical, essentially monomorphic, MHC-I molecules (HLA-E, HLA-F, HLA-G, and HLA-H in humans; H2-M, H2-Q, and H2-T gene products in mice). These MHC molecules bind peptides, with the Ag-binding cleft of the MHC-I molecules being more restricted at the N and C termini in comparison with the open-ended MHC-II molecules

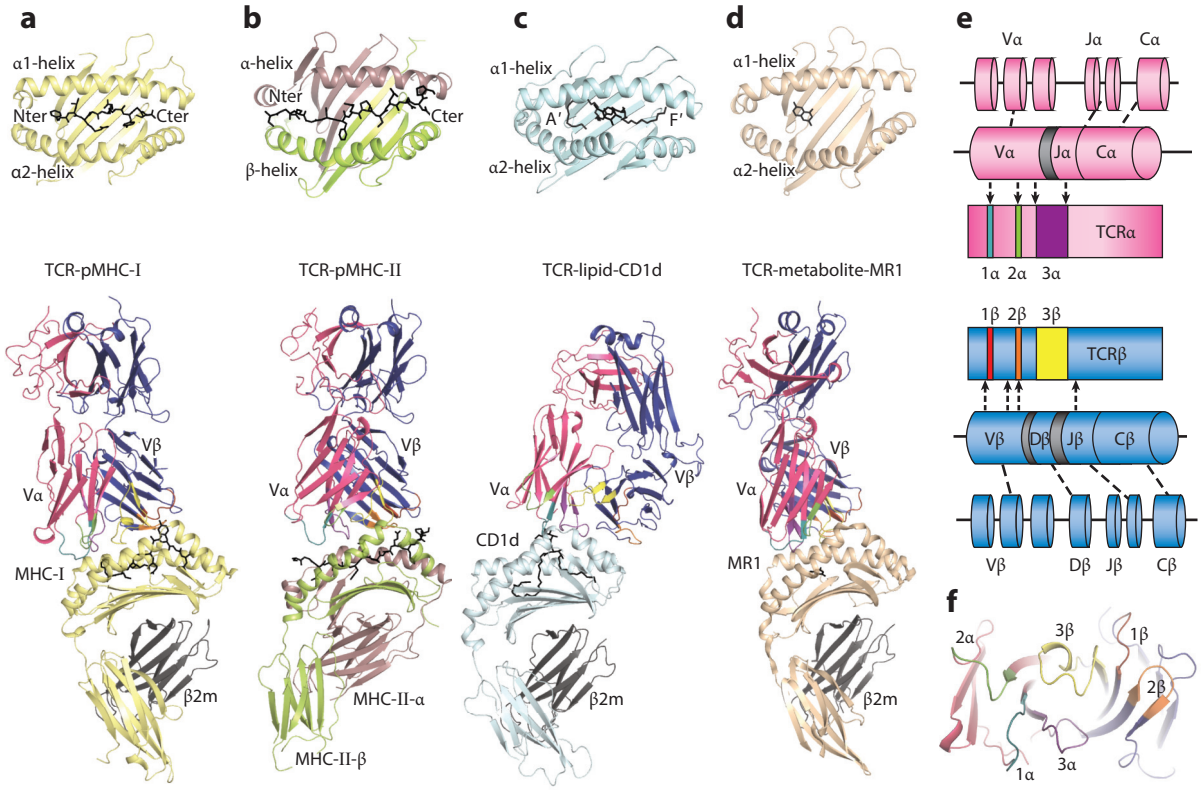

Figure 1

Overview of T cell antigen receptor (TCR) in complex with an array of antigenic complexes: (*a*) TCR-pMHC-I complex, (*b*) TCR-pMHC-II complex, (*c*) TCR-lipid-CD1d complex, and (*d*) TCR-metabolite-MR1 complex, with associated views down the antigen-binding clefts below. Panel (*e*) represents the genetic recombination of TCR genes from the α-chain (*pink*) and the β-chain (*blue*). The complementarity-determining regions (CDRs) 1, 2, and 3 loops are teal, green, and purple for the α-chain and red, orange, and yellow for the β-chain. (*f*) A view of the TCR CDR loops that bind the antigenic complex. Abbreviation: pMHC, peptide-MHC.

(**Figure 1**). As such, MHC-II molecules tend to present longer peptide fragments (>11 amino acids) in comparison with the MHC-I counterparts (8–10 amino acids). The MHC molecules bind the peptides via a series of pockets within the peptide-binding groove, termed A–F pockets in MHC-I and P1–P9 pockets in MHC-II (16). MHC polymorphism is concentrated around the Ag-binding cleft and dictates which, and how, peptides bind to any given MHC molecule. Within the pMHC complexes, the regions of the peptide that are outwardly oriented and solvent exposed can directly contact the TCR, whereas buried residues can indirectly affect TCR binding (17). The nonclassical MHC-I molecules present a more restricted repertoire of peptides and play a key role in innate immunity, although they may mediate T cell responses (18).

The CD1 family of Ag-presenting molecules is subdivided into group 1 (CD1a, CD1b, and CD1c) and group 2 (CD1d) (5). The Ag-binding groove of the CD1 family has two hydrophobic pockets (A′ and F′ pockets) that differ in size, conformation, and extent of solvent exposure, thereby modulating the repertoire of lipids that can bind to any given member (19). Typically, the lipid tails are sequestered within the hydrophobic cleft of CD1, whereas the polar moiety of the lipid protrudes from CD1 to interact with the TCR (**Figure 1**). Regarding MR1, vitamin B–based metabolites are entrapped within MR1, with the ligand barely accessible to the TCR (6)

(**Figure 1**). Thus, the responding TCR has to recognize three different classes of ligands in the context of different Ag-presenting molecules and only has a relatively small region of the Ag to contact. Accordingly, for TCRs to trigger an immune response, needle-in-a-haystack sensing is required, and the immune system has a broad repertoire of TCRs to enable this.

Architecture of the αβTCR

During T cell development in the thymus, functional αβTCR generation requires (*a*) random rearrangement of *variable* (*V*), *diversity* (*D*), and *joining* (*J*) gene segments, and (*b*) random rearrangement of *V* and *J* gene segments from the *TCRβ* and *TCRα* gene loci, respectively. Within the TCR, there are six hypervariable complementarity-determining regions (CDRs) that mediate recognition. The CDR1 and CDR2 regions are encoded within the germ line *TRAV* and *TRBV* genes (20), and the CDR3 regions are formed at the junction of different *V(D)J* gene rearrangements (9) (**Figure 1**).

Establishing a diverse TCR repertoire relies on combinatorial and junctional diversity. Combinatorial diversity arises through the many different permutations and combinations of *V*, *D*, and *J* gene segments, of which there are approximately 43–45 *TRAV*, 50 *TRAJ*, 40–48 *TRBV*, 2 *TRBD*, and 12–13 *TRBJ* functional gene segments. Junctional diversity dramatically expands the TCR repertoire by the lack of accuracy during *V(D)J* gene rearrangement and by the inclusion of nontemplated encoded nucleotides (*N*) at *V(D)J* junctions. Further combinatorial diversity arises from the random pairing of different TCR α-chain and TCR β-chains. From a relatively small number of TCR genes, there are, after thymic selection, approximately 2×10^7 TCRs per human (21). A critical question is how this remarkably diverse TCR repertoire interacts with various MHC-Ag and MHC-I-like-Ag landscapes to affect recognition.

TCR-pMHC-I RECOGNITION

The first αβTCR-pMHC-I structures provided a wealth of information pertaining to this key T cell recognition event (8, 9, 22). The TCR docked above the long axis of the MHC-Ag binding cleft in an approximately diagonal orientation, with the CDR3 loops sitting above the peptide, whereas the germ line–encoded CDR1 and CDR2 loops primarily mediated MHC contacts. The TCR-pMHC-I interface lacked good shape complementarity (namely, a poor fit at this interface), which was in line with the weak (typically 35μM, **Supplemental Table 1**; follow the **Supplemental Materials link** from the Annual Reviews home page at **http://www.annualreviews.org**) affinity of the interaction (23). The CDR3 loops underwent conformational change upon pMHC ligation, which was consistent with the inherent TCR cross-reactivity (10).

Supplemental Material

Since these initial investigations, many structural studies have shed light on key immunological concepts in the context of TCR recognition, including MHC restriction, MHC-I polymorphism, and MHC-I self-tolerance (24); TCR selection (25); cross-reactivity; alloreactivity; T cell–mediated autoimmunity; and allergies (26, 27). Indeed, to date, 34 unique TCR-pMHC-I structures have been determined (**Table 1**). Further, there have been many more closely related ternary complexes solved that vary in terms of (*a*) bound peptide, (*b*) minor differences in the MHC structure, and (*c*) subtle distinctions in TCR gene usage. The structural characteristics of these unique TCR-pMHC-I interactions, including docking angle, buried surface area (BSA), percentage of contributions from the TCR α- and β-chains, the CDR loops, and MHC and peptide, are shown in **Supplemental Table 1** and **Figure 2**. Accordingly, this growing database of TCR-pMHC-I structures has not only addressed many important immunological concepts, but also simultaneously challenged many of the generalities pertaining to TCR-pMHC-I docking that

Table 1 Unique TCR-pMHC-I complex structures

No.	MHC	Peptide[a]	TCR	TRAV[b]	TRBV[b]	TCR-pMHC-I	pMHC-I	TCR	Reference(s)
1	H2-K^b	Self (**INF**DFNTI)	BM3.3	16/DV11*01	1*01	1FO0	1NAN	NA	62, 63
2	H2-K^b	Self (**KVI**TFIDL)	KB5-C20	14–1*01	1*01	1KJ2	1KJ3	NA	64
3	H2-K^b	Synthetic (**WIY**VYRPM)	YAe62	6D-3*01	13–2*01	3RGV	NA	NA	130
4	H2-K^b	Self (**EQY**KFYSV)	2C	9–4*01	13–2*01	2CKB	1LEG	1TCR	9, 22, 45
5	H2-L^d	Synthetic (**QLS**PFPFDL)	2C	9–4*01	13–2*01	2OI9	NA	1TCR	9, 72
6	H2-D^b	Influenza (**SSLE**NFRAYV)	6218	21/DV12*02	29*01	3PQY	1YN6	NA	131, 132
7	H2-K^{bm8}	Synthetic (**SQY**YYNSL)	BM3.3	16/DV11*01	1*01	2OL3	2CLV	NA	81, 133
8	HLA-A*02:01	HTLV (**LLF**GYPVYV)	A6	12–2*02	6–5*01	1AO7	1DUZ	3QH3	8, 134, 135
9	HLA-A*02:01	HTLV (**LLF**GYPVYV)	B7	29/DV5*01	6–5*01	1BD2	1DUZ	NA	68, 134
10	HLA-A*02:01	Self (**ALWGF**FPVL)	AHIII 12.2	12D–2*01	13–3*01	1LP9	1B0G	NA	136, 137
11	HLA-A*02:01	Influenza (**GIL**GFVFTL)	JM22	27*01	19*–01	1OGA	2VLL	2VLM	30, 39
12	HLA-A*02:01	Self (**SLL**MWITQV)	1G4	21*01	6–5*01	2BNQ	NA	2BNU	54
13	HLA-A*02:01	CMV (**NLV**PMVATV)	RA14	24*01	6–5*01	3GSN	3GSO	NA	24, 31
14	HLA-A*02:01	Melanoma (**ELA**GIGILTV)	CD8	12–2*01	30*01	3HG1	1JF1	NA	42
15	HLA-A*02:01	EBV (**GLC**TLVAML)	AS01	5*01	20–1*01	3O4L	3MRE	NA	41
16	HLA-A*02:01	Melanoma (**AAG**IGILTV)	DMF5	12–2*01	6–4*01	3QDJ	3QFD	NA	66, 67
17	HLA-A*02:01	Melanoma (**LAG**IGILTV)	DMF4	35*01	10–3*01	3QDM	2GTW	NA	65, 66
18	HLA-A*02:01	Self (**ALWGP**DPAAA)	1E6	12–3*01	12–4*01	3UTS	3UTQ	NA	55
19	HLA-A*24:02	HIV (**RFP**LTFGWCF)	C1-28	8–3*01	4–1*01	3VXM	3VXO	NA	71
20	HLA-A*24:02	HIV (**RYP**LTFGWCF)	H27-14	21*01	7–9*01	3VXR	3VXN	3VXQ	71
21	HLA-A*24:02	HIV (**RFP**LTFGWCF)	T36-5	12–2*01	27*01	3VXU	3VXO	3VXT	71
22	HLA-B*27:05	HIV (**KRW**IILGLNK)	C12C	14/DV4*02	6–5*01	4G8G	4G9D	NA	34

(*Continued*)

Table 1 (*Continued*)

No.	MHC	Peptide[a]	TCR	TRAV[b]	TRBV[b]	TCR-pMHC-I	pMHC-I	TCR	Reference(s)
23	HLA-B*35:01	EBV (**EPLP**QGQLTAY)	ELS4	1–2*01	10–3*01	2NX5	1ZSD	2NW2	33, 46
24	HLA-B*35:01	EBV (**HPVG**EADYFEY)	TK3	20*01	9*01	3MV7	2FYY	NA	50, 84
25	HLA-B*35:08	EBV (**LPEP**LPQGQLTAY)	SB27	19*01	6–1*01	2AK4	1ZHL	NA	32, 138
26	HLA-B*35:08	EBV (**LPEP**LPQGQLTAY)	SB47	39*01	5–6*01	4JRY	1ZHL	NA	46, 70
27	HLA-B*44:05	EBV (**EENL**LDFVRF)	DM	26–1*02	7–9*01	3DXA	3DX8	3DX9	43, 138
28	HLA-B*44:05	Self (**EEYL**QAFTY)	LC13	26–2*01	7–8*01	3KPS	3KPP	1KGC	37, 73
29	HLA-B*57:03	HIV (**KAF**SPEVIPMF)	AGA1	5*01	19*01	2YPL	2YPK	NA	44
30	HLA-B*08:01	EBV (**FLR**GRAYGL)	LC13	26–2*01	7–8*01	1MI5	1M05	1KGC	29, 36, 37
31	HLA-B*08:01	EBV (**FLR**GRAYGL)	CF34	14/DV4*01	11–2*01	3FFC	1M05	NA	24, 36
32	HLA-B*08:01	EBV (**FLR**GRAYGL)	RL42	12–1*01	6–2*01	3SJV	1M05	3KSN	36, 69
33	HLA-B*51:01	HIV (**TAF**TIPSI)	3B	17*01	7–3*01	4MJI	1E28	NA	40, 139
34	HLA-E*01:03	CMV (**VMA**PRTLIL)	KK50.4	26–1*01	14*01	2ESV	NA	NA	52

Abbreviations: CMV, cytomegalovirus; EBV, Epstein-Barr virus; HIV, human immunodeficiency virus; HLA, human leukocyte antigens; HTLV, human T-lymphotropic virus; MHC, major histocompatibility complex; NA, structure not available; TCR, T cell antigen receptor.

[a]A short name of each peptide appears in bold.

[b]TRAV and TRBV are the Vα and Vβ gene usage for each TCR according to IMGT (**http://www.imgt.org**) nomenclature.

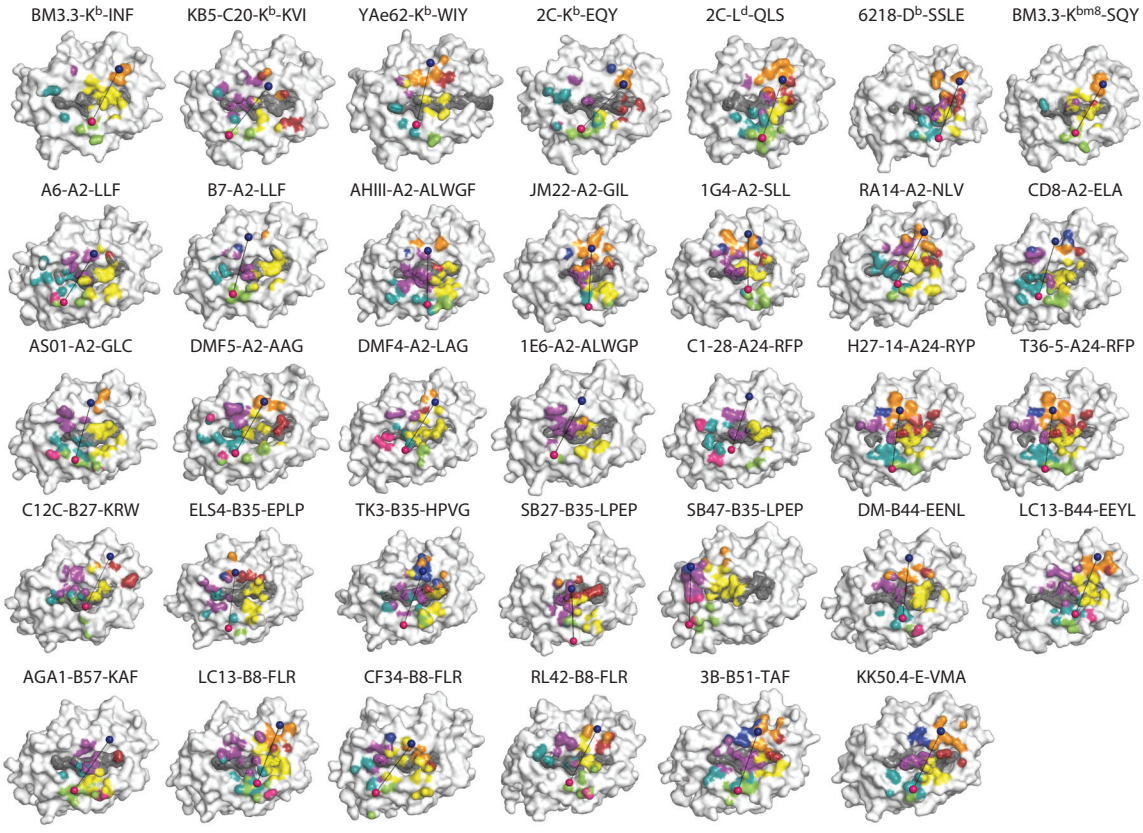

Figure 2

T cell antigen receptor (TCR) footprint onto pMHC-I. TCR footprints onto its specific pMHC-I; MHC-I is in white, and peptides are in gray. The footprints are labeled and ordered as per **Table 1**, from left to right and then top to bottom. The atoms in contact with complementarity-determining regions (CDRs) 1α, 2α, and 3α are teal, green, and purple, respectively, whereas those contacted by CDR 1β, 2β, and 3β are red, orange, and yellow, respectively, as per **Figure 1**. The red and blue spheres represent the centers of mass for the α and β variable domains, respectively. All the complexes are aligned in the same orientation, with a cutoff at 4 Å used to calculate the contacts.

were initially postulated (10). Notably, all TCR-pMHC-I ternary complexes determined to date share an approximate, but common, docking topology in which the Vα-chain is positioned over the α2-helix and the Vβ-chain resides over the α1-helix of MHC-I (**Figure 2**). The significance of, and what governs, this TCR-pMHC consensus docking mode represents key questions in the field. Indeed, the collection of TCR-pMHC-I (and TCR-pMHC-II) structures has allowed the field to form testable hypotheses pertaining to the underlying structural basis of MHC restriction (12, 13, 28).

TCR Bias and MHC-I Recognition

Although TCR diversity is a defining feature in most T cell responses, there are a number of examples of TCR bias in Ag-driven selection (25). Here, biased TRAV and/or TRBV usage, and characteristic CDR3 sequence motifs, can underpin the immune response. There have been a number of structural investigations that have addressed the molecular bases of TCR bias in

the context of infection with cytomegalovirus (CMV), Epstein-Barr virus (EBV), influenza, and human immunodeficiency virus (HIV) (29–34).

Initial insight into TCR bias centered on the T cell response observed in HLA-B*08:01$^+$ individuals toward an EBV determinant (termed FLR; see **Table 1**). The archetypical LC13 TCR-HLA-B*08:01-FLR structure, together with associated mutagenesis studies, showed that the CDR3 loops were the main driving force of the interaction, in a peg-and-notch manner. Here, the P7-Tyr (the peg) protruded into a central cavity (the notch) of the LC13 TCR (29, 35–38). The structure of the biased JM22 TCR bound to an HLA-A*02:01-restricted influenza peptide (termed GIL) revealed a mechanism for recognizing a featureless peptide. Namely, a peg-notch interaction was also observed; but here, an Arg within the CDR3β loop (the peg) resided within a notch that is formed by a small cavity within the pHLA-I (30, 39). An analogous situation was observed in a biased TCR-pHLA-B*51:01 complex (40). These observations indicated that biased TCR usage was a mechanism to enable the recognition of otherwise featureless pMHC-I landscapes. A combination of structural and reverse genetics approaches in a mouse model of influenza directly supported this hypothesis (25).

It is now clear, however, that biased TCR usage is not attributable only to the recognition of featureless landscapes, as TCR bias has been observed in the T cell response to canonical peptides and peptides (>11 amino acids) that protrude from the Ag-binding cleft (32, 41). To illustrate, the structure of the AS01 TCR complexed to HLA-A*02:01 presenting a nonameric peptide showed how the biased TRAV5 and TRBV20-1 gene usage related to specific pHLA-I contacts (41). Similarly, biased TCR usage against an HLA-A*02:01-restricted HCMV 9-mer Ag predominates in immunocompromised patients. Here, the underlying TCR bias was attributed to recognition of three hot spots of the peptide Ag (31). In addition to TCR bias in viral immunity, biased TRAV12-2 gene usage against an HLA-A*02:01-restricted melanoma peptide and its heteroclitic analogue has been described (42). In the ensuing ternary complex, the TRAV12-2 bias was related to the CDR1α loop making a focused network of interactions with the HLA and N-terminal region of the peptide. Thus the germ line TCR fine bias is partly attributable to peptide-mediated contacts (42).

However, it is not always the case that TCR bias reflects the need to engender specificity-governing contacts with the pMHC-I. A number of factors can affect T cell repertoire selection, including convergent recombination, the host's MHC-I haplotype, viral mutations, and the requirement for particular Vα-Vβ pairings that enable optimal TCR-pMHC-I binding (25). The latter scenario was suggested in the study of HLA-B*27:05$^+$ individuals infected with HIV-1 clade B. Here, the crystal structure of a TRBV6-5/TRBJ1-1$^+$ TCR-HLA-B*27:05 bound to an HIV epitope showed that the TRBV6-5 chain made suboptimal contacts with HLA-B*27:05, suggesting that biased TRBV6-5 gene usage may reflect preferred *TRBJ1-1* or TCR α-chain pairing (34). Clearly, understanding the mechanisms that shape T cell repertoire selection remains a key challenge.

TCR Recognition and MHC-I Polymorphism

In mice, the classical *MHC-I* locus is the site of the *H2-K*, *H2-D*, and *H2-L* alleles, whereas in humans it is occupied by the *HLA-A*, *HLA-B*, and *HLA-C* alleles, of which there are greater than 8,000 different allotypes. Classical MHC-I alleles, which can differ by up to 30 amino acids, and more closely related, polymorphic alleles that differ by just 1–2 amino acids can profoundly affect the repertoire of bound peptides, pMHC-I structure, and, consequently, TCR recognition. It is noteworthy that despite this great diversity the unique TCR-pMHC-I structural database encompasses only 12 distinct MHC-I allotypes. Indeed, this database is skewed toward 11 TCR-pHLA-A2 complexes and 4 TCR-pH2-K^b ternary complexes (**Table 1**).

TCR recognition of disparate MHC-I allomorphs invokes a diverse spectrum of TCR-pMHC-I docking modes (**Figure 2**, **Supplemental Table 1**), making it challenging, from a structural perspective, to ascribe clear principles explaining the monomorphic and polymorphic MHC residues that govern the docking mode. However, structural studies concerning TCR recognition of micropolymorphic MHC-I molecules have been informative in addressing how a few amino acids can affect MHC-I restriction and biological outcome (32, 43–45).

Supplemental Material

For example, three overlapping EBV-derived peptides, a 9-mer, an 11-mer, and a 13-mer, bind equally well to HLA-B*35:01; however, CTL responses in HLA-B*35:01$^+$ individuals are focused on the 11-mer, whereas the 13-mer is restricted to HLA-B*35:08$^+$ individuals (46). The HLA-B*35:01 and HLA-B*35:08 allomorphs differ by a single polymorphism at position 156 (Leu/Arg), which is buried within the Ag-binding cleft. This polymorphism controls selection of the 13-mer peptide by HLA-B*35:08 by favoring an electrostatic interaction between Arg156 and the peptide that does not occur in HLA-B*35:01 because of the aliphatic Leu156. The structure of the SB27 TCR-HLA-B*35:08-13-mer complex revealed the fine specificity of MHC-I restriction against this superbulged peptide (32, 47). Here the rigid, bulged 13-mer peptide thwarted the scope of TCR binding to HLA-B*35:08, in that the TCR-pMHC-I interface contained twice as many peptide-mediated contacts as MHC-I interactions. This limited MHC contact is in contrast to the more extensive MHC-I footprint of TCRs that recognized peptides of canonical length (32) (**Figure 2**). Nevertheless, the SB27 TCR was restricted to HLA-B*35:08 and bound to HLA-B*35:01-13-mer with threefold lower affinity. This difference was due to Leu156 in HLA-B*35:01 altering a region of the α2-helix contacted by the SB27 TCR, a region that represents an energetic hot spot for this interaction. In contrast, structural analysis of a different TCR (clone ELS4) that bound to an HLA-B*35:01-11-mer complex indicated that this peptide was more flexible and was flattened upon TCR ligation. Here, Arg156 in HLA-B*35:08 appeared to prevent the bulldozing (flattening) of the 11-mer peptide, thereby demonstrating a clear example of how micropolymorphisms can affect MHC restriction (33).

Similarly, the T cell response toward HLA-B*57:01 presenting an HIV-derived peptide (KAF) is finely controlled by HLA micropolymorphism. HLA-B*57:03, which differs from HLA-B*57:01 by two positions (Asn114/Asp and Tyr116/Ser), caused a fivefold lower affinity interaction with a defined KAF-HLA-B*57:03-reactive TCR (AGA1) (44). These buried polymorphisms affect the ability of the peptide to undergo conformational change upon TCR ligation. Similarly, the immunogenicity to an EBV determinant (EENL) is dictated by micropolymorphisms within the HLA-B44 family, in which HLA-B*44:05 is preferentially recognized in comparison with the same epitope when presented by HLA-B*44:02 or HLA-B*44:03 (43). These HLA-B44 allomorphs differ at two buried positions (HLA-B*44:02: Asp116/Asp156; HLA-B*44:03: Asp116/Leu156; HLA-B*44:05: Tyr116/Asp156) (48). The crystal structure of a TCR-HLA-B*44:05-EENL complex, together with the HLA-B*44:05/03/02-EENL binary structures, shows how these buried polymorphisms affect the conformation and mobility of the bulged region of the peptide, a region that undergoes conformational change upon TCR ligation (49). Thus, the HLA-B44 polymorphisms affect peptide mobility, and TCR induced fit of the peptide (49). Similarly, micropolymorphism-induced structural dynamics of a 12-mer peptide appears to skew an HLA-B*35:01-restricted T cell response in favor of HLA-B*35:08 (50, 51).

In addition to *MHC* polymorphism, the *TCR* locus is extremely polymorphic, with allele variation being linked to both autoimmunity and protective immunity (50). However, the structural basis of how TCR polymorphism affects pMHC recognition is limited to one example—namely, the crystal structure of a TCR (TK3) bound to HLA-B*35:01 presenting an EBV peptide provided insight into the preferential usage of the *TRBV9*01* allele over the *TRBV9*02* allele; these are differentiated by one residue (Gln55/His). This polymorphism, located within the framework

region, exclusively contacted the EBV peptide. The TCR Gln55/His polymorphism changed the charge complementarity at the TK3 TCR-pHLA-B*35:01 interface, which caused the TRBV9*02^{+} TCR (His55) to exhibit a reduced affinity and reactivity toward this pMHC-I complex (50). It remains to be established whether MHC and TCR polymorphism can affect the MHC-restricted response via other mechanisms.

TCR Recognition of Nonclassical MHC-I Molecules

Whereas nonclassical MHC-I molecules play a major role in innate immunity, there is a growing appreciation that these Ag-presenting molecules can also participate in T cell–mediated responses. For example, the role of HLA-E is to present MHC-I leader sequences to control NK cell–mediated lysis (18). However, CMV has thwarted this innate sensing mechanism by encoding CMV mimics of MHC-I leader sequences; nevertheless, this engenders a T cell–mediated response against a CMV peptide presented by HLA-E. The crystal structure of a TCR (KK50.4)-HLA-E-CMV peptide complex provided insight into a monomorphic MHC-I-restricted T cell response (52, 53). Although the TCR adopted a docking mode above HLA-E that was comparable to classical TCR-pMHC-I interactions, there were a few distinguishing features of the TCR-pHLA-E interaction (**Figure 2**). Namely, the CDR2β loop played a dominant role, and all three CDRβ loops focused on position 8 of the CMV peptide, which defined the sole point of discrimination between self and nonself. However, structural studies on nonclassical TCR-pMHC-I interactions are limited to this one example, and as such, many more structural studies are required to understand whether there is a fundamental difference underpinning TCR recognition of polymorphic MHC-I and monomorphic MHC-1 molecules.

TCR and MHC-I Plasticity and Cross-Reactivity

The relationship between TCR plasticity and T cell cross-reactivity has been gleaned from determining the structures of the nonliganded TCR and pMHC-I structures in conjunction with the respective ternary complexes. TCR plasticity was first shown in the 2C TCR-H2-K^{b}-dEV8 interaction, in which the dEV8 peptide represents a weak agonist self-ligand (22). Here, three of the 2C TCR CDR loops changed conformation upon ligation to avoid clashes with the MHC-I or maximize contacts with the pMHC-I ligand. As the regions of the 2C TCR that underwent the large conformational change corresponded, in part, to the region of the TCR that contacted the peptide, the structural comparisons highlighted how the hypervariable regions of the 2C TCR could mold around the hypervariable peptide cargo.

Comparison of an unliganded and MHC-I-bound LC13 TCR structure revealed that the germ line–encoded CDR1α and CDR2α loops, in addition to the CDR3 loops, underwent plastic deformation upon ligation (29, 37). However, CDR loop movement is not a general feature of TCR recognition. For example, comparison of a nonliganded TCR (1G4) with that bound to an HLA-A*02:01 molecule presenting a tumor epitope (SSL) revealed that the TCR possessed a preformed cavity that was ideally suited to bind the tumor epitope (54). Analogously, an autoreactive TCR (1E6) showed limited conformational movement upon binding to HLA-A*02:01 presenting a preproinsulin-derived epitope (55).

Upon TCR-pMHC-I engagement, the pMHC-I is relatively fixed. However, some structural studies have shown that pMHC-I plasticity, principally relating to peptide malleability, can play a key role in induced-fit TCR recognition (8, 33, 43). Peptides (>10 amino acids) that protrude from the MHC-I cleft can exhibit an increased flexibility, owing to a lack of stabilizing contacts within either the peptide itself or inter-MHC-I contacts (56). For example, three studies have demonstrated how peptide plasticity was a central feature underpinning a TCR recognition event

(33, 43, 50). Interestingly, the relative positioning of the Vα-Vβ domains were changed in two systems investigated (DM TCR-HLA-B*44:05-EENL, and the JM22 TCR-HLA-A*02:01-GIL; 39, 43). The biological significance of such Vα-Vβ movements is unclear, but it may relate to TCR signaling events.

Conformational changes in the MHC and peptide were seen when the A6 TCR engaged an HLA-A*02:01-restricted peptide (Tel1p) (57). Namely, the structure of A6 TCR-HLA-A*02:01-Tel1p revealed that the conformation of the peptide mimicked the structure of the Tax (LLF) peptide within the A6 TCR-HLA-A*02:01-LLF complex. However, the respective ternary complexes did not perfectly mirror each other, as differences in the CDR loops, the peptide, and the HLA-A*02:01 molecule itself were apparent. Specifically, HLA-A*02:01 had a more open conformation in the A6 TCR-HLA-A*02:01-Tel1p structure, thereby revealing that TCR cross-reactivity can be related to plasticity in the MHC-I molecule (57).

Structural studies on altered peptide ligands (APLs) have shown that the TCRs recognize APLs in a very similar manner to that of their respective cognate complexes (58–60). However, flexibility at the TCR-pMHC-I interface, which could encompass movements in the CDR loops, the peptide, or the MHC residues, was required to accommodate the different APLs. Moreover, voids at the TCR-pMHC-I interface were associated with weaker affinity, with the filling of such voids correlating with enhanced TCR recognition (60). From biophysical measurements, it was apparent that T cell signaling outcome did not necessarily correlate with either TCR affinity or the half-life of the interaction (60).

Understanding TCR recognition of APLs is potentially useful in the context of tumor immunotherapy. This was demonstrated upon TCR (1G4) recognition of the HLA-A*02:01-SSL and its variant SSL-C9V, in which the C-terminal cysteine was replaced by valine (54). The 1G4 TCR enveloped the central region of the SSL epitope (54). Curiously however, the SSL-C9V variant resulted in enhanced T cell killing, and it was not immediately apparent how a mutation buried within the F pocket of HLA-A*02:01 could affect TCR recognition. The two ternary complexes shed light on the impact of the APL. Namely, the P9-Val sat slightly deeper in the F pocket of HLA-A*02:01, the effect of which was propagated toward a slight repositioning of the central region of the peptide, which subsequently affected 1G4 TCR recognition. Accordingly, APLs that are generated to stabilize MHC contacts can also indirectly affect TCR recognition (54).

Further insight into TCR cross-reactivity arose from examining TCRs in complex with closely related pMHC-I complexes, as observed in the 2C TCR recognizing a self-peptide (termed EQY; **Table 1**) bound to H2-K^{b} and H2-K^{bm3}. H2-K^{b} and H2-K^{bm3} molecules differ at two positions (Asp77/Ser and Ala89/Lys) that are located within the Ag-binding cleft, with this allelic variation resulting in the negative selection of 2C T cells in H-2K^{bm3+} mice (61). The 2C TCR recognizes the H2-K^{b} and H2-K^{bm3} complexes similarly; however, subtle changes in the BSA and shape complementarity were observed. This was related mostly to the buried Asp77/Ser polymorphism, which indirectly affected TCR recognition by altering the conformation of the peptide (61). Structural studies on another murine TCR (BM3.3) have also revealed how one TCR can bind three different pMHC-I complexes (62–64). Namely, the BM3.3 TCR has been solved in complex with H2-K^{b} presenting two different peptides (VSV8 and pBM1), and the H2-K^{bm8} molecule bound to another peptide (pBM8, termed SQY; **Table 1**) (62–64). These three structures show how alterations of the CDR loops enable the BM3.3 TCR to adopt the same overall docking on these three different pMHC-I complexes. Notably, the CDR3α loop of the BM3.3 TCR changes shape markedly upon binding to these three different peptides.

TCR cross-reactivity toward HLA-A*02:01-restricted epitopes from the melanoma-Ag (MART1, termed AAG and LAG; **Table 1**) has also been investigated. Here two TCRs (DMF4 and DMF5) that differ in their TRAV-TRBV and CDR3 usage cross-reacted onto closely related

and overlapping nonameric and decameric peptides (65–67). The DMF5 TCR cross-reacted onto these peptides by adopting a similar docking mode over HLA-A*02:01. In contrast, the DMF4 TCR docking differed by a 15° rotation upon binding the 9-mer and 10-mer complexes. The contacts between the CDR3β loop of the DMF4 TCR and the P4–P8 region of these two peptides were conserved, thereby highlighting the peptide centricity of this interaction. Notably, the germ line–encoded CDRα loops contacted HLA-A*02:01 differently, thereby illustrating how the peptide changes the docking mode even when the TCR and MHC-I are identical.

Varied TCR Usage and pMHC-I Recognition

A hallmark of adaptive immunity is the ability of a diverse T cell repertoire to respond to a given Ag restricted to a specific MHC-I allotype. Accordingly, it was of interest to establish how varied TRAV and/or TRBV usage resulted in recognition of the same pMHC-I complex. This has been established in four distinct settings, HLA-A*02:01-Lff, HLA-A*24:02-RFP, HLA-B*08:01-FLR, and HLA-B*35:08-LPEP (24, 68–71) (**Table 1**, **Figure 2**). A comparison of two distinct TCRs (A6 and B7) bound to HLA-A*02:01-Lff provided the first insight into how diverse TCR usage can affect pMHC-I recognition (**Figure 2**, **Supplemental Table 1**). Although the A6 and B7 TCRs shared the same TRBV chain, they differed in TRAV gene usage (68). These TCRs docked onto HLA-A*02:01-Lff similarly, although the TCR β-chain of the B7 TCR tilted toward HLA-A*02:01-Lff more than the A6 TCR. Although there were common contact regions between the two ternary complexes, differences at the respective interfaces resulted in altered responses to peptide analogues (68).

Supplemental Material

The structures of three TCRs bound to HLA-A*24:02 presenting an HIV epitope have been determined (71). The three TCRs (H27-14, T36-5, and C1-28) exhibited different TCR α- and β-chain usage yet adopted a broadly similar docking mode (**Table 1**, **Figure 2**). Nevertheless, within this common footprint, the C1-28 TCR exhibited a much-reduced contribution from the TCR β-chain. The nature of the interatomic contacts with the viral determinant varied between the three TCRs, thereby providing a molecular basis for the ability of the T cells to respond to viral escape mutants (71). The crystal structures of two distinct TCRs binding to the HLA-B*35:08-LPEP complex have revealed how TCR gene usage can result in contrasting docking footprints atop a common pMHC-I (70). Namely, while one TCR (SB27) sat above the peptide bulge making limited contacts with HLA-B*35:08, the other TCR (SB47) essentially avoided the central bulged region of the peptide and formed an extensive footprint at the extreme N-terminal end of HLA-B*35:08 (**Figure 2**) (70).

Altered TCR gene usage in the context of self-HLA tolerance has been investigated. As the LC13 TCR alloreacts on HLA-B44 (discussed below), these clonotypes are deleted in *HLA-B8*$^{+}$*B44*$^{+}$ individuals, presumably to avoid self-reactivity (24, 69). Consequently, in *HLA-B8*$^{+}$*B44*$^{+}$ individuals a markedly different TCR repertoire is used to recognize HLA-B*08:01 bound to a dominant EBV determinant (FLR; **Table 1**). Two distinct TCRs selected in *HLA-B8*$^{+}$*B44*$^{+}$ individuals (CF34 and RL42) were shown to ligate HLA-B*08:01 in a significantly different manner compared with LC13 TCR docking (**Figure 2**) (24, 69). The RL42 TCR ligated centrally over HLA-B*08:01-FLR, reflecting a shift in the TCR specificity toward the P1 and P8 positions of the peptide (69) compared with the P7 focus of LC13 TCR. In contrast, the CF34 TCR footprint was located over the N terminus of HLA-B*08:01, a location that correlated with the surface-exposed polymorphisms distinguishing HLA-B*08:01 from HLA-B*44:02/03/05, and reflected the heightened sensitivity this TCR exhibited toward the P1 position of the peptide (31). These ternary complexes indicated that to avoid self-MHC reactivity, the TCRs see the differences between the HLA-B8 and HLA-B44 allomorphs. Consistent with this notion, this suggested

that alloreactivity could be attributed more generally to spotting the similarities between HLA allomorphs.

T Cell Alloreactivity

Structural studies have provided the first glimpses into the molecular basis of T cell alloreactivity (72, 73). Alloreactivity manifests as T cell–mediated organ rejection and graft-versus-host disease (GVHD) and is an important immunological concept to understand (14).

A central question was whether the peptide or the MHC-I molecule was the principal driver of alloreactivity (14). The MHC-I-centric model of allorecognition proposes that T cells focus on the polymorphic MHC-I residues, whereas the peptide-centric model postulates that the TCR recognizes the similarities between the self-MHC-I and allogeneic MHC-I molecules while reacting to the allopeptide as foreign. Two structural studies have showcased how these two models of alloreactivity operate. Firstly, the structures of the 2C TCR bound to H2-K^b-EQY and to its allogeneic ligand, H2-L^d-QLS, and peptide variants thereof, have been elucidated (72, 74). H2-K^b and H2-L^d differ by 31 amino acids, 7 of which are accessible to the TCR. Moreover, there was limited sequence similarity between the 8-mer self-peptide and 9-mer allopeptide. Comparison of these ternary complexes revealed two different docking modes (**Figure 2**). Namely, in comparison with the 2C TCR-H-2K^b-EQY complex, the 2C TCR α- and β-chains were repositioned by 30° and 15°, respectively, upon recognition of H2-L^d-QLS (72). This resulted in the germ line–encoded CDR loops of the 2C TCR adopting differing positions atop the cognate and alloreactive complexes. Hence, this study indicated an MHC-centric basis of alloreactivity (72).

In contrast, studies on the LC13 TCR showed that alloreactivity could operate via peptide-dependent molecular mimicry (73). Namely, the LC13 TCR alloreacts onto members of the HLA-B44 family bound to a naturally presented allopeptide (EEYL; **Table 1**). HLA-B*44:05 differs from HLA-B*08:01 by 25 amino acids, of which 5 polymorphic positions are surface exposed. Further, the HLA-B*08:01-restricted viral peptide and the HLA-B44-bound allopeptide differed in their amino acid sequence. Nonetheless, the alloreactive ternary complexes mimicked that of the cognate ternary interaction. Although the viral peptide and allopeptide displayed differing conformations in their respective binary complexes, they adopted very similar conformations in the LC13 TCR–bound state, thereby showing an induced-fit form of molecular mimicry. Most notably, although the sequences of the two peptides varied, they shared an aromatic residue at position 7, which participated in very similar interactions with the LC13 TCR (73). In addition, this study provided a basis for understanding why the LC13 TCR recognized HLA-B*44:05 and HLA-B*44:02 but did not alloreact onto HLA-B*44:03. These observations raise the question of whether divergent docking modes or molecular mimicry will be the general mechanism underlying allorecognition. Recently, a yeast-display approach has indicated that focused peptide-centric mimicry is the principal mechanism of T cell cross-reactivity (26). To formally establish this, more cognate and associated alloreactive TCR-pMHC-I structures will be required.

TCR-pMHC-II RECOGNITION

The first glimpse of how TCRs engage pMHC-II was achieved with the structure of the mouse D10 TCR bound to an albumin-derived peptide presented by I-A^k (75; **Table 2**). The D10 bound its pMHC-II ligand with a distinctive orthogonal binding mode, which suggested that diagonal versus orthogonal binding differentiated between the CD8 (diagonal) and CD4 (orthogonal) lineages. The TCR-pMHC-I and TCR-pMHC-II structural database clearly shows this is incorrect. Presently, there are 22 unique TCR-pMHC-II complexes (**Table 2**), and analogous to TCR-pMHC-I recognition, they all adopt a consensus docking polarity; namely, the TCR α-chain

Supplemental Material

is positioned over the β-chain α-helix of the MHC-II, whereas the TCR β-chain resides above the α-chain α-helix of the MHC-II (**Figure 3**). The characteristics of the unique TCR-pMHC-II interfaces are depicted in **Supplemental Table 2**. The majority of these studies have been focused primarily on understanding TCR-pMHC-II recognition in the context of TCR-MHC bias and aberrant TCR reactivity.

TCR-MHC-II Bias

A compelling notion holds that the TCR-pMHC interaction is underpinned by basic rules whereby the TCR is thought to be preprogrammed to dock the MHC platform using conserved footprints or codons (28, 76). Central to this theory is the proposed subdivision of binding whereby germ line–encoded regions of the TCR bind to the MHC, while the CDR3 loops focus on the peptide cargo. Evidence for TCR-MHC bias has been observed whereby TCRs bearing a common TRBV13 element dock on different I-A^b, I-A^k, or I-A^u (and MHC-I targets) with overlaying modalities (**Figure 3**). Namely, the conserved docking included pairwise interaction motifs between CDR1, CDR2, and MHC (75–78) or conserved germ line–encoded TCR loop positioning on the MHC platform (78, 79). Principal in these observations were two tyrosine residues within the CDR2β loop of the TRBV13$^+$ TCRs. Notably, a structural alignment of numerous TCR complexes with H-2L^d has shown an invariant positioning of the TRAV9-4-encoded CDR2α on H2-L^d (K.C. Garcia, unpublished observations). As the TCR-pMHC structural database grows it is evident that the rules underlying evolutionarily based interactions are not straightforward. For instance, the same TCR that binds different peptides presented by the same MHC can have considerably different binding footprints (13, 80, 81), an observation characterized as peptide editing (13). In addition, the CDR3 composition and structure can override codon interactions, a process termed CDR3 editing (13, 76). Structural evidence for codon override via CDR3 editing includes divergent docking in spite of common TRAV22 elements (82, 83) and divergent docking in spite of common TRBV9 elements (50, 84, 85). Also blurring the lines of evolutionarily based interactions is the observation that TCRs have built-in flexibility and can produce compensatory contacts when key conserved MHC contact sites are mutated (12). Regardless, these investigations have provided testable hypotheses for other TRAV and/or TRBV gene elements and contributed important additions to the TCR-pMHC-II structural database (13). Thus, it will be interesting to establish the extent of the generality pertaining to conserved germ line–encoded docking modalities.

Aberrant TCR Reactivity

The structural determination of numerous autoreactive TCR-pMHC-II complexes has yielded three different, yet synergistic, theories of why CD4 T cells can escape negative selection and initiate pathology. The off-center-binding hypothesis was proposed following the determination of the ternary structure of a TCR-pMHC-II complex derived from a multiple sclerosis (MS) patient (86). Here, the Ob.1A12 TCR interacting with a myelin-derived peptide presented by HLA-DR2 revealed that the TCR docked over the N-terminal flank of the pMHC-II platform (**Figure 3**). A similar docking strategy was seen when the same TCR bound to a cross-reactive peptide derived from *Escherichia coli* (87). The docking of these complexes contrasted with the central docking of an antimicrobial MHC class II ternary complex (88). However, it is established that such atypical TCR-pMHC-II docking modes are not the sole mechanism of autoreactivity. For instance, the autoreactive TCRs, 172.10 (89), 1934.4, and C119 (76), from mice undergoing experimental autoimmune encephalomyelitis (EAE), bind their I-A^u-restricted myelin-derived peptide ligands in a central fashion. Likewise, within the MHC-I system, the autoreactive 1E6 TCR derived from a type 1 diabetes patient (55) binds its insulin-derived pMHC-I ligand canonically, whereas some

Table 2 Unique TCR-pMHC-II complex structures

No.	MHC	Peptide	TCR	TRAV*	TRBV*	TCR-pMHC-II	pMHC-II	TCR free	Reference(s)
1	HLA-DQ1	MBP 85–99 (ENPVVHFFKNIVTP)	Hy.1B11	13–1*02	7–3*01	3PL6	NA	NA	94
2	HLA-DQ2.5	Gliadin-α2 peptide (APQPELPYPQPGS)	JR5.1	26–1*01	7–2*01	4OZF	NA	NA	97
3	HLA-DQ2.5	Gliadin-α1 peptide (QPFPQPELPYP)	S2	4*01	20–1*01	4OZI	NA	NA	97
4	HLA-DQ8	Gliadin-α1 (SGEGSFQPSQENP)	SP3.4	26–2*01	9*01	4GG6	2NNA	4GG8	85
5	HLA-DR1	Triosephosphate isomerase (GELIGILNAAKVPAD)	G4	22*01	5–8*01	4E41	NA	4E42	82
6	HLA-DR1	Triosephosphate isomerase (GELIGTLNAAKVPAD)	E8	22*01	6–6*01	2IAN	NA	2IAL	83
7	HLA-DR1	Influenza hemagglutinin (PKYVKQNTLKLAT)	HA1.7	8–4*01	28*01	1FYT	NA	4GKZ	88, 94
8	HLA-DR1	DR52c-pHIR (QHIRCNIPKRISA)	ANI2.3	8–3*01	19*01	4H1L	4H25	NA	140
9	HLA-DR1	*E. coli* protein (DFARVHFISALHGSG)	Ob.1A12	17*01	20–1*01	2WBJ	NA	NA	87
10	HLA-DR2b	MBP 85–99 (ENPVVHFFKNIVTP)	Ob.1A12	17*01	20–1*01	1YMM	NA	NA	86
11	HLA-DR2a	MBP 89–101 (VHFFKNIVTPRTPG)	3A6	9–2*02	5–1*01	1ZGL	NA	NA	96
12	HLA-DR4	MBP 111–129 (FSWGAEGQRPGFG)	MS2-3C8	26–2*01	20–1*01	3O6F	NA	NA	91
13	HLA-DP2	M2-Be^{2+}	AV22	9–2*01	5–1*01	4P4K	NA	NA	98
14	$I\text{-}A^b$	3K peptide (FEAQKAKANKAV)	B3K506	6–7/DV9*02	13–3*01	3C5Z	1LNU	NA	77, 141
15	$I\text{-}A^b$	3K peptide (FEAQKAKANKAV)	YAe62	6D–3*01	13–2*01	3C60	1LNU	NA	77, 141
16	$I\text{-}A^b$	3K peptide (FEAQKAKANKAV)	2W20	14–2*01	13–2*01	3C6L	1LNU	NA	77, 141
17	$I\text{-}A^b$	3K peptide (FEAQKAKANKAV)	809.B5	14D–3/DV8*02	13–2*01	3RDT	1LNU	NA	100, 141
18	$I\text{-}A^{g7}$	Hen egg lysozyme 11–27 (GAMKRHGLDNYRGYSLG)	21.30	4–2*01	13–3*01	3MBE	NA	NA	142
19	$I\text{-}A^u$	MBP Ac1-11 (RGGASQYRPSQ)	1934.4	6D–7*01	13–2*01	2PXY	1K2D	2Z35	76, 90
20	$I\text{-}A^u$	MBP Ac1-11 (SRGGASQYRPSQ)	172.10	14–3*01	13–2*01	1U3H	1K2D	NA	89, 90
21	$I\text{-}E^k$	MCC peptide cytochrome *c* (ADLIAYLKQATKG)	2B4	4D–4*02	26*01	3QIB	NA	3QJF	143
22	$I\text{-}A^k$	Conalbumin peptide (GNSHRGAIEWEGIESG)	D10	14D–2*01	13–2*01	1D9K	NA	1BWM	75, 144

Abbreviations: HLA, human leukocyte antigens; MBP, myelin basic protein; MHC, major histocompatibility complex; NA, free structure not available; TCR, T cell antigen receptor.
*TRAV and TRBV are the Vα and Vβ gene usage for each TCR according to IMGT (**http://www.imgt.org**) nomenclature.

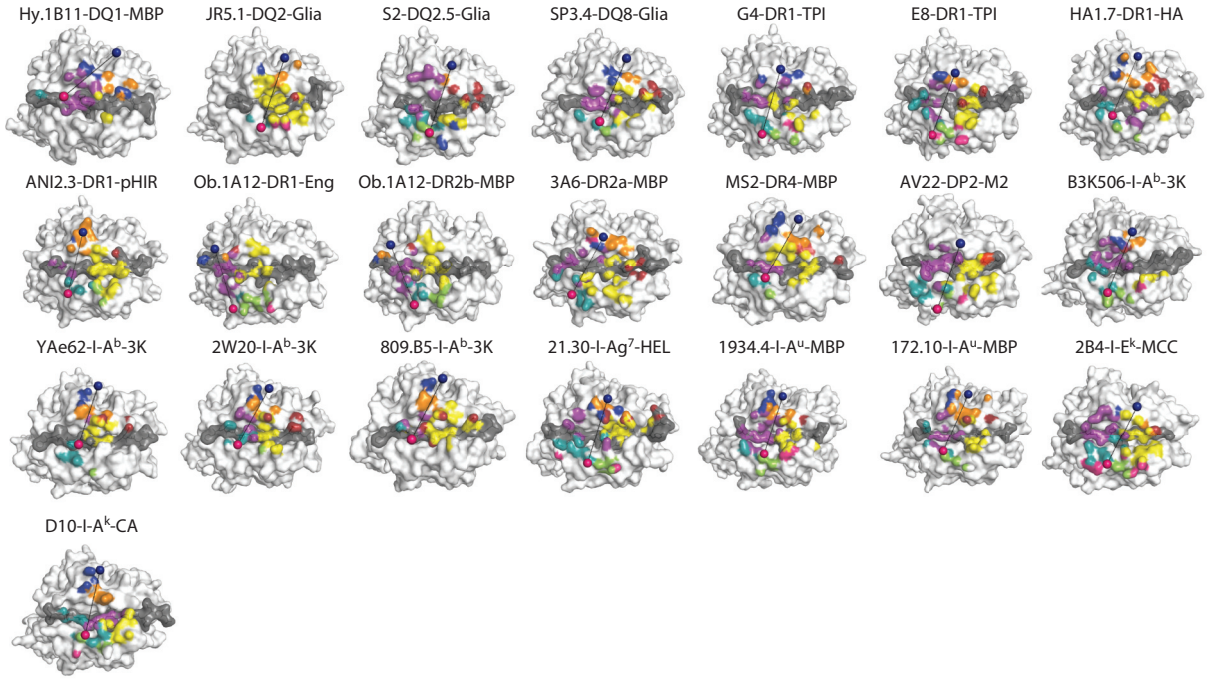

Figure 3

T cell antigen receptor (TCR) footprint on pMHC-II. TCR footprints on its specific pMHC-II; MHC-II is in white and peptide is in gray. Complexes are labeled and ordered according to **Table 2**, from left to right and then top to bottom. Color scheme as per **Figure 2**.

antimicrobial TCRs bind MHC-I within extreme N-terminal docking modes (**Figure 2**). Thus it is likely that both autoreactive and antimicrobial TCRs will dock along the full length of the MHC platform.

Given that autoreactive TCR-pMHC-II complexes can bind in the canonical manner, a second mechanism was proposed—i.e., that defects in the binding affinity between the peptide and MHC underlie pathology (3). For TCRs associated with EAE in mice (89, 90), and MS in humans (91), the affinity between peptide and MHC-II is particularly weak (92) in spite of canonical TCR docking and high TCR-binding affinities (**Supplemental Table 2**). Thus, these autoreactive T cells can bind well but are functionally limited by the short-lived and unstable nature of their cognate self-pMHC-II targets.

Supplemental Material

The hot spot mimicry model of aberrant TCR reactivity proposes that rather than spreading contacts over a large number of peptide residues (82, 83), autoreactive TCRs concentrate their binding energy on a very small area of the peptide. The consequence of this focused footprint is that the TCR may be prone to heightened cross-reactivity and have a greater chance of accidental off-target pathology (93). An example of hot spot mimicry arose from a TCR (Hy.1B11) from an MS patient that bound a myelin-derived peptide presented by HLA-DQ1 (94). While positioned conventionally over the center of the peptide, the Hy.1B11 TCR was markedly tilted toward the MHC α1-helix. This docking modality resulted in only one of four germ line–encoded CDR loops contacting the MHC and only a single CDR3 loop contacting the peptide (**Figure 3**). Moreover, this CDR3α-mediated contact drove cross-reactivity toward two distinct peptides (95). Similarly, another autoreactive TCR (Ob.1A12) exhibited a focused contact hot spot over the peptide N

terminus that allowed cross-reactivity between a myelin peptide and an *E. coli* peptide that exhibited little sequence homology (87). Another autoreactive TCR (3A6), from an MS patient and specific for a myelin-derived peptide presented by HLA-DQ2, also exhibited an extremely focused and small peptide footprint (96). Immense capacity for peptide cross-reactivity has been established in both mouse and human TCR-pMHC-II systems (26), where TCR cross-reactivity is likely achieved through superior tolerance for substitutions to peptide residues outside of the TCR contact footprint. Collectively, as initially observed in the LC13 TCR system (73), these studies indicate that focused peptide-centric mimicry can underpin aberrant T cell reactivity.

Studies of T cell recognition in celiac disease, an autoimmune-like disorder triggered by posttranslational modification of dietary-derived gluten, have concentrated on the disease susceptibility alleles *HLA-DQ2* and *HLA-DQ8* and three gluten determinants, DQ2.5-glia-α1a, DQ2.5-glia-α2, and DQ8-glia-α1 (**Table 2**) (85, 97). Biased TCR usage was observed to underpin the response to these Ags. The structure of the prototypic SP3.4 TCR specific for HLA-DQ8-glia-α1 revealed a peptide-centric and canonical docking mode (85) with the TRBV9 bias related to two germ line–encoded hot spots. Similarly, analyses of three TCRs specific for the HLA-DQ2-restricted epitopes provided a basis for gliadin epitope specificity, with the extent of TRAV-HLA-DQ2-mediated contacts toward DQ2.5-glia-α2 being affected by the CDR3β loop (97). However, despite the TCR bias, an Arg residue not encoded in the germ line and within the CDR3 loop was observed to act as the lynchpin in mediating the HLA-DQ8- and HLA-DQ2-restricted response (85, 97).

Recently, the structural basis of chronic beryllium disease has been elucidated (98). This disease is associated with HLA-DP2, where the Be^{2+} ion was buried within the Ag-binding cleft and made contacts with the peptide. As such, the TCR did not directly contact the Be^{2+} ion. However, the binding of Be^{2+} caused structural perturbations in HLA-DP2, which subsequently affected TCR recognition. These findings are analogous to HLA-linked drug hypersensitivities, where abacavir, by binding to HLA-B*57:01, modulates the self-peptide repertoire, thereby triggering an aberrant immune response (99). Given the central role T cells play in HLA-linked immune-related diseases, we clearly need to gain a greater understanding of how autoreactive TCRs engage their HLA-II molecules.

MHC-II/MHC-I Cross-Reactivity

The molecular basis of MHC cross-class recognition has been established using the mouse YAe62 model system that expresses only one pMHC-II complex (91). Namely, the YAe62.8 TCR structure has been determined in complex with the cognate I-A^b complex and a cross-reactive H2-K^b complex. The YAe62.8 TCR cross-reactivity was attributable to pMHC-induced adjustments in TCR interactions, with the plasticity of the TCR permitting pMHC-I recognition. Interestingly, conservation of CDR2β contacts across MHC-I and MHC-II was observed. In an extension of the same system, the interactions between the α- and β-chains of a TCR can also be a key factor in determining MHC restriction and cross-reactivity (100). A structural comparison of the YAe62.8 TCR and another TCR (J809.B5), bound to I-A^b-3K, highlighted that even though these TCRs shared the same TCR β-chain, the energetics underpinning these interactions with the MHC differed (100). However, the structural basis of MHC-I/MHC-II cross-reactivity in a more physiological setting remains to be established.

LIPID RECOGNITION

The structural basis of TCR recognition of CD1-Ag is presently limited to the NKT TCR-CD1d-Ag axis (15) (**Table 3**, **Figure 4**, **Supplemental Table 3**).

Supplemental Material

Table 3 Innate-like TCR complex structures

Type I								
No.	**CD1d**	**Antigen**	**TRAV**	**TRBV**	**PDB**	**Ag-CD1d**	**TCR**	**Reference(s)**
1	mCD1d	α-GalCer	11*02	1*01	3TO4	1Z5L	NA	105, 145
2	mCD1d	α-GalCer	11*02	13–2*01	3HE6	1Z5L	2Q86	104, 145, 146
3	mCD1d	α-GalCer	11*02	29*01	3HE7	1Z5L	NA	104, 145
4	mCD1d	α-GalDAG (microbial)	11*02	13–2*01	3O9W	NA	NA	115
5	mCD1d	SMC124	11*02	13–2*01	3TVM	NA	NA	147
6	mCD1d	PI (self-lipid)	11*02	19*01	3QI9	NA	NA	107
7	mCD1d	iGb3 (self-lipid)	11*02	19*01	3SCM	2Q7Y	NA	109, 146
8	mCD1d	α-GlcCer	13D–3*01	13–3*01	3RUG	1Z5L	3AXL	106, 145
9	hCD1d	α-GalCer	10*01	25–1*01	2PO6	1ZT4	2EYS	101, 148, 149
10	hCD1d	Lyso-PC (self-lipid)	10*01	25–1*01	3TZV	3U0P	3TYF	111
11	hCD1d	α-GalCer	17*01	25–1*01	4EN3	1ZT4	NA	108, 149
Type II								
No.	**CD1d**	**Antigen**	**TRAV**	**TRBV**	**PDB**	**Ag-CD1d**	**TCR**	**References**
12	mCD1d	Sulfatide	7D–4*01	3*01	4EI5	2AKR	4EI6	117, 150
γδTCR								
No.	**CD1d**	**Antigen**	**TRDV**	**TRGV**	**PDB**	**Ag-CD1d**	**TCR**	**Reference(s)**
13	hCD1d	Sulfatide	TRDV1*01	TRGV4*01	4MNG	4MQ7	4MNH	7
14	hCD1d	α-GalCer	TRDV1*01	TRGV5*01	4LHU	1ZT4	4LFH	120, 149
MAIT								
No.	**MR1**	**Antigen**	**TRAV**	**TRBV**	**PDB**	**Ag-MR1**	**TCR**	**Reference(s)**
1	hMR1	6-FP	1–2*01	6–1*01	4L4T	4GUP	NA	121, 122
2	hMR1	RL-6-Me-7-OH	1–2*01	6–1*01	4L4V	NA	NA	122
3	hMR1	Acetyl-6-FP	1–2*01	6–1*01	4PJ5	NA	NA	127
4	hMR1	5-OE-RU	1–2*01	6–1*01	4NQE	NA	NA	128
5	hMR1	5-OP-RU	1–2*01	6–1*01	4NQC	NA	NA	128
6	hMR1	5-OP-RU	1–2*01	6–4*01	4PJ7	NA	NA	127
7	hMR1	5-OP-RU	1–2*01	20–1*01	4PJ8	NA	4DZB	127
8	bMR1	rRL-6-CH_2OH[b]	1–2*01	6–1*01	4LCC	NA	NA	124
9	bMR1	6-FP[b]	1–2*01	6–1*01	4IIQ	NA	NA	123

Abbreviations: Ag, antigen; α-GalCer, α-galactosylceramide; α-GalDAG, α-galactosyldiacylglycerol; b, bovine; 5-OE-RU, 5-(2-oxoethylideneamino)-6-D-ribitylaminouracil; 5-OP-RU, 5-(2-oxopropylideneamino)-6-D-ribitylaminouracil; h, human; iGb3, isoglobotrihexosylceramide; Lyso-PC, lysophosphatidylcholine; m, mouse; NA, structure not available; PI, phosphatidylinositol; 6-FP, 6 formylpterin; SMC124, analogue of α-GalCer; TCR, T cell antigen receptor.

[a]TRAV and TRBV are the Vα and Vβ gene usage for each TCR according to the IMGT nomenclature.

[b]Ag was modelled in the structure but not formerly identified.

Type I NKT TCR Recognition

Type I NKT cells are, for the most part, comprised of a fixed TCR α-chain (TRAV10-TRAJ18 in humans) and a biased TCR β-chain repertoire (TRBV25-1 in humans). Type I NKT cells are also defined by their reactivity toward α-galactosylceramide (α-GalCer), and owing to its potent stimulatory properties and broad recognition by these cells, this compound is considered the archetypal type I NKT ligand (15). However, type I NKT TCRs can recognize a broad repertoire of lipids, including synthetic, self, and foreign Ags that are presented by CD1d (15). These Ags

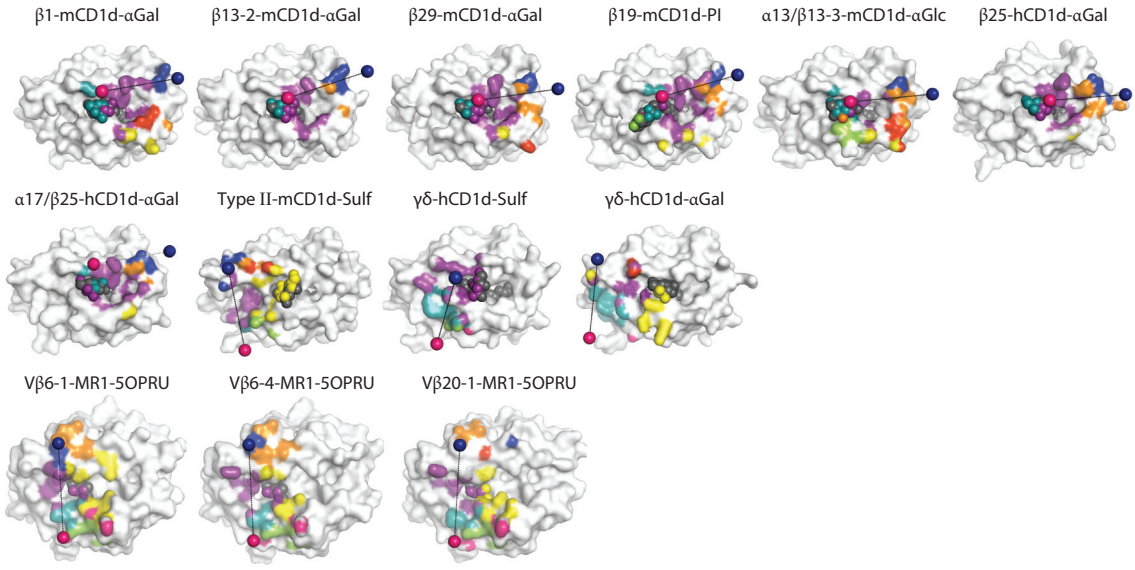

Figure 4

T cell antigen receptor (TCR) footprint on CD1d-lipid and MR1-metabolite. TCR footprints on CD1d (top two rows) and MR1 molecules (bottom row). The surface of CD1d or MR1 is in white, and the lipid or metabolite is represented by gray spheres. The complexes are labeled according to **Table 3**. The most representative TCR-lipid-CD1d complexes have been selected. Color scheme as per **Figure 2**.

collectively differ in the size and charge of their polar headgroups and the length and saturation of the fatty acid chain(s). Below we summarize type I NKT TCR recognition of self, foreign, and synthetic Ags.

The first structure of a NKT TCR-CD1d-α-GalCer complex established the broad paradigm for type I NKT TCR recognition (101). All subsequent type I NKT TCR ternary complexes, including those from humans and mice, adopt a very similar docking mode (15, 101). These complexes are markedly different from all TCR-peptide-MHC complexes studied thus far, whereby the type I NKT TCR docked parallel to the Ag-binding cleft over the F′ pocket of CD1d (101) (**Figure 4**). At the type I NKT TCR-CD1d-α-GalCer interface, the CDR1α and CDR3α loops contacted the sugar moiety of α-GalCer (101), thereby providing an understanding of type I NKT TCR specificity toward this ligand. The CDR3α-CD1d contacts were principally electrostatic, whereas Leu99α caps a "hydrophobic roof" on CD1d. The TCR β-chain contacts were dominated by the CDR2β loop, which converged to interact with the F′ roof of CD1d. Mutagenesis studies highlighted the key roles played by CDR2β and CDR3α loops in this NKT TCR-CD1d interaction (102, 103).

Impact of NKT TCR Repertoire on CD1d Binding

Given that alterations in the NKT TCR repertoire affected functional outcome, it was established how variations in the NKT TCR α- and β-chains affected CD1d-Ag binding (104–106). Within the consensus parallel docking mode, differences in the NKT TCR-CD1d interactions were apparent, with the CDRβ loops "collaborating" to enable binding (104). For example, for some NKT TCRs, the CDR1β and CDR3β loops played a more prominent role in binding CD1d. The

greater involvement of the CDR3β loop was consistent with this loop enabling Ag-independent CD1d autoreactivity (discussed below) (107).

In addition to variations within the TCR β-chain, type I NKT subsets exist with variations in the TRAV/TRAJ gene usage that affect ligand specificity. For example, a mouse TRAV13D3-TRAJ50^{+} NKT cell population exhibited greater reactivity toward α-GlcCer than α-GalCer, whereas human TRAV10^{-} NKT cells reacted poorly with α-GlcCer compared with α-GalCer (106, 108). Structural analysis of ternary complexes of a mouse TRAV13D3-TRAJ50^{+} NKT TCR and a human TRAV17-TRAJ18^{+} NKT TCR showed differences at the respective NKT TCR-CD1d-Ag interfaces, thus providing insight into the molecular basis for the differing ligand specificities of these NKT cell subsets (106, 108).

Type I NKT TCR Self-Ag Recognition

Type I NKT cell recognition of self-lipid Ags, which include phospholipids and β-linked glycolipids, is implicated in a number of diseases. Self-Ag reactivity of type I NKT cells can be modulated via the CDR3β loop interacting directly with CD1d in an Ag-independent manner (107). Generally, mammalian glycolipids constitute β-linked glycolipids, whose headgroup protrudes outward from CD1d. The structure determination of type I NKT TCRs in complex with β-GalCer and isoglobotrihexosylceramide (iGb3) provided insight into β-linked glycolipid recognition (109, 110). Namely, the NKT TCRs flatten the β-linked glycolipid headgroups into a conformation resembling the α-linked Ags. This flattening of the ligand is coincident with a lowering of affinity toward the CD1d-β-linked Ag complex. The structures of the type I NKT TCR in complex with CD1d-Gb3 and CD1d-β-LacCer revealed that the terminal sugar moiety is a critical determinant governing the antigenicity of iGb3 by making compensatory interactions with CD1d itself, thereby counterbalancing the energetic penalty of flattening the ligand (109).

Phospholipids, an abundant component of cell membranes, appear, in general, to be poor agonists for the majority of type I NKT cells. The structures of type I NKT TCRs in complex with CD1d-phosphatidylinositol and CD1d-lysophosphatidylcholine have shown how the type I NKT TCR can accommodate phospholipids within the consensus type I NKT TCR docking mode (107, 111). In both situations, the phospholipid was reorientated upon type I NKT TCR binding. Why phospholipids are generally such poor Ags for type I NKT cells is unclear but may reflect the lack of electrostatic complementarity between the TRAJ18-encoded CDR3α loop and the phospholipid headgroup itself.

Synthetic Ags

α-GalCer can unpredictably initiate T_H1- and T_H2-type immune responses, which is an undesirable characteristic for a future therapeutic. Thus, α-GalCer analogues have been developed with a view to polarizing the immune response. A series of structural studies on α-GalCer analogues, termed altered glycolipid ligands (AGLs), have provided an understanding of type I NKT TCR fine specificity and how subtle modifications in the AGLs can exert a profound effect on biological outcome (112, 113). Notably, fine specificity between human and mouse type I NKT cells toward AGLs can differ markedly, so care must be taken in extrapolating from these two species (114). AGLs with modifications at the glycosyl headgroup can directly affect TCR recognition, the effects of which are dependent upon the nature of the substituent. Moreover, although the lipid tails of CD1d-restricted ligands are not directly accessible to the type I NKT TCR, their modification can nevertheless affect type I NKT cell recognition (112). Thus, buried modifications can exert their effect on type I NKT TCR recognition in a similar manner to that of buried MHC polymorphisms

that transmit their effects on TCR recognition. Collectively, these studies suggest that the affinity of the type I NKT TCR-CD1d-Ag interaction is a reliable measure of an AGL's potency.

Microbial Ligands

The type I NKT TCR can recognize microbial Ags, including α-glycuronosylceramides and α-glycosyldiacylglycerols (115, 116). Notably, the α-glycosidic linkage generally represents a microbial signature. Analogous to the recognition of β-linked ligands, type I NKT TCR recognition of these diverse microbial Ags can be achieved by reorientating the headgroup and reshaping the F′ pocket upon CD1d-Ag binding (115). Moreover, type I NKT TCR repertoire diversity also facilitates the recognition of some microbial glycolipids. Interestingly, modifications within the diacylglycerol chains can determine which lipid tails reside within the A′ or F′ pockets of CD1d, which subsequently affects polar headgroup positioning and hence antigenicity of the ligand itself (116). Clearly it will be important to establish the spectrum of microbial lipid Ags and the degree of their potency toward type I NKT cells.

Type II NKT TCR Recognition

Our understanding of type II NKT TCR recognition of CD1d is much more limited. However, it is established that type II NKT cells, unlike type I NKT cells, exhibit a diverse TCR repertoire. Moreover, type II NKT cells do not respond to α-GalCer and are activated by Ags, such as sulfatide, which are generally not recognized by type I NKT cells (15). Nevertheless, type II NKT cells appear to be more abundant than type I NKT cells in humans and are thought to play functional roles distinct from those of type I NKT cells.

The structure of a type II NKT TCR binding to CD1d-sulfatide and CD1d-lysosulfatide revealed that the type II NKT TCR docked orthogonally over the A′ roof of CD1d, and thus type II NKT TCR recognition can be markedly different from type I NKT TCR recognition (**Figure 4**) (117, 118). Moreover, this interaction was dominated via the CDR3α loop and the CDR3β loop contacting CD1d and the sulfated headgroup, respectively. It remains to be established whether other type II NKT TCRs will adopt differing docking modes on CD1d-Ag, although a type II NKT TCR mutagenesis study indicated that this might be the case (117). Regardless, the initial structural snapshot suggested that type II NKT TCR recognition is fundamentally distinct from type I NKT TCR recognition and that this likely relates to differing functional properties of type II NKT cells.

γδTCR Recognition of CD1d

Similar to αβTCRs, γδTCRs are assembled from the products of multiple gene segments. Specifically, the TCR γ-chain comprises the Vγ and Jγ gene products that join to the γ constant (Cγ) domain, whereas Vδ, Dδ, and Jδ gene products fuse to the δ constant (Cδ) domain to form the TCR δ-chain. The γδTCR comprises six CDR loops, and because our structural understanding of γδTCR recognition is limited, the relative role of these CDR loops in enabling recognition is unclear. Previously it was shown how γδTCRs recognize the stress-inducible MHC-I-like receptor, T22, a molecule that does not present Ag (119). Although γδ T cells have been reported to bind lipids and metabolites, the structural basis of Ag-dependent γδTCR recognition was unclear. Recently, two studies provided insight into how a TRDV1$^+$ γδTCR binds to a CD1d-Ag complex, thereby providing the first portrait of how αβTCRs and γδTCRs can interact with the same Ag-presenting molecule (7, 120). Firstly, the interaction between a TRDV1$^+$ γδTCR

and CD1d-α-GalCer was established. This γδTCR docked orthogonally over the A′ roof of CD1d. Here, the CDR1δ loop and the CDR3δ loop dominated the interactions at the γδTCR-CD1d interface, with a cluster of Trp residues within the CDR1δ loop playing a principal role in enabling germ line–encoded recognition of CD1d. In contrast, the CDR3γ loop exclusively contacted α-GalCer, thereby indicating how sequence variations within the CDR3γ loop could affect Ag specificity (120). Secondly, a TRDV1$^+$ γδTCR-CD1d-sulfatide complex was determined (7). Here, the γδTCR was positioned over the A′ roof of CD1d, but the γ-chain did not participate in the interaction with CD1d-sulfatide (7). The Trp-rich germ line–encoded CDR1δ loop played a major role in mediating contacts with CD1d, although the actual CD1d-CDR1δ contact zone between these two γδTCR ternary complexes differed (7, 120). The CDR3δ loop of the sulfatide-reactive γδTCR, in addition to contacting CD1d, was the sole region that interacted with the sulfatide ligand. These studies underscore how CDR3 variability can affect Ag specificity and highlight how γδ T cells can utilize a variety of TCR-δ and TCR-γ interactions to detect different Ag-Ag-presenting molecule complexes.

METABOLITE RECOGNITION

Supplemental Material

Mucosal-associated invariant T cells (MAITs) are an innate-like T cell population whose TCR is restricted to MR1 (**Figure 4**, **Table 3**, **Supplemental Table 3**). The human MAIT TCR typically comprises an invariant TCR α-chain (TRAV1-2 joined to TRAJ33, or less commonly TRAJ12 and TRAJ20) with an array of TCR β-chains (commonly TRBV20 or TRBV6) in which the CDR3β loop is hypervariable (6). Structural and metabolomics-based studies showed that MR1 could present vitamin B–based metabolites, including a photodegradation product of folic acid (6-formylpterin, 6-FP) and riboflavin precursors (7-hydroxy-6-methyl-8-D-ribityllumazine, RL-6-Me-7-OH; 6,7-dimethyl-8-D-ribityllumazine, RL-6,7-diMe; and reduced 6-hydroxymethyl-8-D-ribityllumazine, rRL-6-CH_2OH) (121). The structure of the MR1-6-FP complex confirmed that MR1 adopted the MHC-I fold (**Figure 1**), forming a constricted Ag-binding cleft that was well suited to bind small molecule metabolites. Here, 6-FP was enveloped by an aromatic cradle and formed a Schiff base with Lys43 of MR1 (121). Although 6-FP could bind MR1, it did not activate MAIT cells, leading to the speculation that the additional ribityl tail on riboflavin-based precursors represented an additional moiety required for MAIT TCR binding that would result in MAIT cell activation. The significance of MAIT cells recognizing riboflavin-based precursors is that it represents a potential self/nonself discrimination mechanism, given that mammals can only acquire riboflavin from dietary sources, whereas many bacteria and yeast synthesize riboflavin (121).

A number of structural studies have provided insight into how the MAIT TCR can recognize MR1 bound to vitamin B–based metabolites (**Table 3**, **Supplemental Table 3**). The MAIT TCR was solved in complex with MR1 presenting the 6-FP ligand and the weak agonist RL-6-Me-7-OH (122). The overall docking of these two complexes was essentially the same, and indeed similar to that of xenoreactive MAIT TCR–MR1 complexes (with undefined Ags bound), thereby underscoring the evolutionarily conserved nature of this interaction (**Figure 4**) (123, 124). The human MAIT TCR docked centrally and orthogonally atop MR1, in which the invariant TRAV1-2-TRAJ33 chain primarily contacted MR1. In contrast, the CDR1β and CDR2β loops played a lesser role in contacting MR1 (125, 126). Nevertheless, the CDR3β loop extensively interacted with MR1, implying that its variability may affect MAIT TCR recognition. Indeed, it has recently been established how variations within the CDR3β loop result in modulating direct contacts with the Ag (127). The MAIT TCR docking mode was consistent with mutagenesis

studies that showed that only a few MAIT TCR α-chain residues were critical for recognition, whereas the TCR β-chain was largely dispensable (126).

The MAIT TCR made limited direct contacts with RL-6-Me-7-OH and no direct contacts with 6-FP, consistent with the nonagonist activity of this folate-based ligand. However, the CDR3α loop of the MAIT TCR acted like a wedge to pry open the MR1-binding cleft, thereby enabling a direct contact with the ribityl tail of RL-6-Me-7-OH (122). Notably, whereas 6-FP formed a Schiff base with MR1, RL-6-Me-7-OH did not, and its lumazine ring was reorientated approximately 75° with respect to 6-FP within the MR1 cleft. This indicates a degree of promiscuity in the MR1 binding pocket, suggesting that other ligands may be able to bind in unpredictable ways (122).

Although these findings provided a basis for understanding MAIT ligand antigenicity, they did not explain the potency of synthetic rRL-6-CH_2OH or the origins of the ligand itself, as rRL-6-CH_2OH is not a metabolite found in the riboflavin pathway. It was subsequently shown that the riboflavin precursor 5-amino-ribityluracil (5-A-RU) forms an adduct with other metabolites, such as glyoxal and methylglyoxal, to generate potent MAIT cell Ags (128). Moreover, it was shown that MR1 captures the transitory species, including 5-(2-oxopropylideneamino)-6-D-ribitylaminouracil (5-OP-RU), that formed Schiff base complexes with MR1 (128). Thus, MR1 captures unstable pyrimidine intermediates formed from condensation of the riboflavin precursor 5-A-RU with glyoxal or methylglyoxal. In isolation, these intermediates are converted to the more stable lumazines. Taken together, these studies showed that pyrimidine adducts are a metabolic signature of riboflavin-synthesizing microbes that stimulate MAIT cells. Remaining central questions require addressing whether other ligands can bind MR1 and, if so, how the MAIT TCR can recognize such MR1-Ag complexes.

DISCUSSION AND FUTURE DIRECTIONS

Our understanding of TCR Ag recognition has progressed markedly in the last few years, with the TCR representing a versatile scaffold that interacts with peptides, lipids, and metabolites. The field has progressed mostly in the area of peptide-mediated immunity, with greater than 50 unique TCR-pMHC structures now determined (**Tables 1** and **2**, **Figures 2** and **3**). Clearly, neither the shape complementarity statistic nor BSA at the TCR-pMHC interfaces is a reliable indicator of the affinity of the interaction (**Supplemental Tables 1** and **2**). Emerging evidence is collectively indicating that there is greater variation in the features underpinning TCR-pMHC-I recognition compared with TCR-pMHC-II binding (**Figure 5**). As both MHC-I and MHC-II are polymorphic, this difference may possibly be related to the MHC-II-restricted peptide exhibiting less conformational freedom in comparison with the MHC-I-bound peptide. These studies have provided insight into the fundamental basis of protective immunity, factors that shape the TCR repertoire, the impact of MHC and TCR polymorphism, TCR cross-reactivity, alloreactivity, autoimmunity, and allergy. Collectively these studies have enabled theories pertaining to MHC restriction to be postulated and tested. Although TCR-pMHC structural studies had provided an enticing glimpse of pairwise TCR-MHC motifs, other studies have shown such motifs can be blurred on accord of variation in the peptide, the MHC allotype, and TCR gene usage. For example, in MHC-I immunity, the same gene segments (TRBV1, TRBV13-2, TRBV6-5, TRAV12-2, and TRAV21) have been observed to interact with multiple pMHC-I complexes, but with no conservation in the docking footprint related to that particular gene segment being observed (**Table 1**, **Figure 2**). Similarly, in MHC-II-mediated immunity the TRBV20-encoded gene segment has markedly differing interactions with the MHC-II in three distinct settings (**Table 2**, **Figure 3**). On average, the two CDR3 loops play the most prominent role at the TCR-pMHC interface (44% and 49%

Supplemental Material

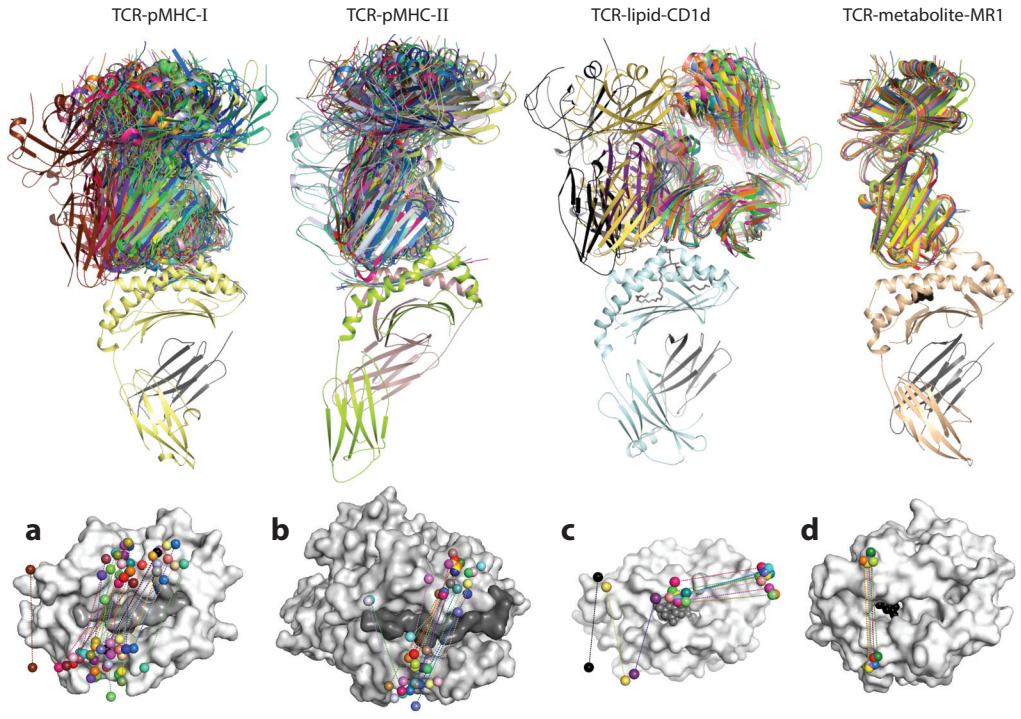

Figure 5

Overview of the structural database of T cell antigen receptor (TCR)-antigen complexes. The (*a*) TCR-pMHC-I, (*b*) TCR-pMHC-II, (*c*) TCR-lipid-CD1d, and (*d*) TCR-metabolite-MR1 structures have been aligned together via their antigen-binding cleft, with the TCRs represented in different colors. The lower portions of the panels show the docking of the different TCRs on (*a*) pMHC-I, (*b*) pMHC-II, (*c*) lipid-CD1d, and (*d*) metabolite-MR1 complexes. In the top row, each TCR is depicted in a distinct color: MHC-I (*yellow*), MHC-II (*green* and *light pink*), CD1d (*light blue*), MR1 (*light brown*), and β2m (*gray*). In the bottom row are the surface representations of the antigen-presenting molecules (*white*) and the centers of mass (*spheres*) for the α-chains and β-chains of the TCRs. The color of the sphere is unique for each TCR, as in top panels.

Supplemental Material

BSA for MHC-I and MHC-II interactions). The germ line–encoded regions, while contacting the MHC, can also make key contacts with the peptide cargo (**Supplemental Tables 4** and **5**). Conversely, the CDR3 loops, in addition to contacting the peptide, frequently contact the MHC (**Supplemental Tables 4** and **5**). For example, the CDR3 loops, on average, contribute 35% and 39% BSA toward the MHC-I and MHC-II molecules (respectively) alone, whereas on average, the germ line–encoded regions contribute 29% and 33% BSA toward contacting the MHC-I- and MHC-II-restricted peptide, respectively. Individual examples of TCR-pMHC interactions also clearly show that the contribution the CDR3 loops and germ line–encoded regions make toward contacting the MHC and peptide can be >50% BSA (**Supplemental Tables 4** and **5**). The median TCR-pMHC-I docking angle is 63.2°, but this value ranges from 37° to 90° (**Supplemental Table 1**). Similarly, the TCR-pMHC-II docking angle ranges from 44° to 115°, with a median value of 76.4° (**Supplemental Table 2**). Thus, the parameters surrounding MHC restriction are quite varied at the multifactorial TCR-pMHC interface, although it is clear that the peptide itself plays a key role in enabling and dictating TCR docking. Any future investigations regarding MHC bias should try to actively account for this peptide parameter as well as the role of the

germ line–encoded regions contacting the peptide, and CDR3-MHC-specific contacts. Despite these impressive advances in TCR-pMHC structures, the coverage of HLA space remains thin. Our understanding of nonclassical MHC-I molecules in adaptive immunity remains marginal, and how TCRs interact with other receptors (129) is unknown. The linkage of the *MHC-II* locus to autoimmunity and subsequent TCR recognition is largely underexplored structurally, as is the MHC-II-restricted antimicrobial response. Clearly the field needs to determine many more TCR-pMHC structures to further evaluate the factors that determine MHC restriction and the ensuing biology.

The field of lipid recognition has progressed, and it appears that the factors underpinning type I NKT TCR recognition are fundamentally different from those underpinning TCR-pMHC binding, with type I NKT TCRs appearing to behave as an innate-like pattern-recognition receptor with little variation in overall docking mode (**Figure 5**) (15). The rare glimpse of type II NKT TCR recognition seems to more closely resemble peptide-mediated recognition. However, our understanding of TCR-lipid interactions is limited to CD1d, and the structural basis of group 1 CD1 recognition by TCRs is a key area of future investigation. Interestingly, γδTCRs have been shown to recognize CD1d in an Ag-dependent manner (7, 120), and the extent and mode of recognition of other Ag-presenting molecules need to be evaluated.

In the context of metabolite immunity, it has recently been established that the MAIT TCR can bind vitamin B–based metabolites restricted to MR1, thereby revealing a new class of Ag that can lead to αβTCR activation (**Figure 5**). Whether MR1 can bind to other Ags remains a central question; if so, the nature of the responding TCR repertoire would be important to ascertain. More broadly, given that many metabolites are unique to microbes, the field of metabolite-specific T cell–mediated immunity is an exciting and important new frontier of investigation.

Ultimately, regardless of the nature of the Ag, how TCR recognition relates to intracellular signaling remains unclear, and this is principally due to our lack of understanding of the TCR-CD3 interaction, before and after Ag ligation. Nevertheless, recently it has been proposed that the consensus TCR-pMHC docking topology may be related to the need to engage the coreceptors (80). However, the orientation of these nonproductive signaling TCR-pMHC complexes falls within the range of that observed in TCR-pMHC docking (**Supplemental Tables 1** and **2**), suggesting that other parameters regarding nonproductive engagement may be at play. Accordingly, there remains much fundamental T cell biology to be explored structurally in numerous axes of health and disease, and collective acquisition of such illuminating data will translate to development of novel therapeutics and diagnostics to monitor and treat patients with diseases related to immunity.

Supplemental Material

DISCLOSURE STATEMENT

The authors are not aware of any affiliations, memberships, funding, or financial holdings that might be perceived as affecting the objectivity of this review.

ACKNOWLEDGMENTS

We thank K.C. Garcia and J.W. Kappler for sharing unpublished data. This research was supported by grants from the National Health and Medical Research Council of Australia (NHMRC), the Australian Research Council (ARC), the Roche Organ Transplantation Research Fund (ROTRF), and the Cancer Council of Victoria. D.I.G. was supported by an NHMRC Senior Principal Research Fellowship; J.J.M. was supported by an NHMRC CDF fellowship; S.G. and S.J.T. were supported by ARC Future Fellowships; J.R. was supported by an NHMRC Australia Fellowship.

LITERATURE CITED

1. van der Merwe PA, Dushek O. 2011. Mechanisms for T cell receptor triggering. *Nat. Rev. Immunol.* 11:47–55
2. Bharadwaj M, Illing P, Theodossis A, Purcell AW, Rossjohn J, McCluskey J. 2012. Drug hypersensitivity and human leukocyte antigens of the major histocompatibility complex. *Annu. Rev. Pharmacol. Toxicol.* 52:401–31
3. Yin Y, Li Y, Mariuzza RA. 2012. Structural basis for self-recognition by autoimmune T-cell receptors. *Immunol. Rev.* 250:32–48
4. Zinkernagel RM, Doherty PC. 1997. The discovery of MHC restriction. *Immunol. Today* 18:14–17
5. Brigl M, Brenner MB. 2004. CD1: antigen presentation and T cell function. *Annu. Rev. Immunol.* 22:817–90
6. Birkinshaw RW, Kjer-Nielsen L, Eckle SB, McCluskey J, Rossjohn J. 2014. MAITs, MR1 and vitamin B metabolites. *Curr. Opin. Immunol.* 26C:7–13
7. Luoma AM, Castro CD, Mayassi T, Bembinster LA, Bai L, et al. 2013. Crystal structure of Vδ1 T cell receptor in complex with CD1d-sulfatide shows MHC-like recognition of a self-lipid by human γδ T cells. *Immunity* 39:1032–42
8. Garboczi DN, Ghosh P, Utz U, Fan QR, Biddison WE, Wiley DC. 1996. Structure of the complex between human T-cell receptor, viral peptide and HLA-A2. *Nature* 384:134–41
9. Garcia KC, Degano M, Stanfield RL, Brunmark A, Jackson MR, et al. 1996. An αβ T cell receptor structure at 2.5 Å and its orientation in the TCR-MHC complex. *Science* 274:209–19
10. Rudolph MG, Stanfield RL, Wilson IA. 2006. How TCRs bind MHCs, peptides, and coreceptors. *Annu. Rev. Immunol.* 24:419–66
11. Yin L, Scott-Browne J, Kappler JW, Gapin L, Marrack P. 2012. T cells and their eons-old obsession with MHC. *Immunol. Rev.* 250:49–60
12. Burrows SR, Chen Z, Archbold JK, Tynan FE, Beddoe T, et al. 2010. Hard wiring of T cell receptor specificity for the major histocompatibility complex is underpinned by TCR adaptability. *PNAS* 107:10608–13
13. Garcia KC, Adams JJ, Feng D, Ely LK. 2009. The molecular basis of TCR germline bias for MHC is surprisingly simple. *Nat. Immunol.* 10:143–47
14. Felix NJ, Allen PM. 2007. Specificity of T-cell alloreactivity. *Nat. Rev. Immunol.* 7:942–53
15. Rossjohn J, Pellicci DG, Patel O, Gapin L, Godfrey DI. 2012. Recognition of CD1d-restricted antigens by natural killer T cells. *Nat. Rev. Immunol.* 12:845–57
16. Adams EJ, Luoma AM. 2013. The adaptable major histocompatibility complex (MHC) fold: structure and function of nonclassical and MHC class I–like molecules. *Annu. Rev. Immunol.* 31:529–61
17. Theodossis A, Guillonneau C, Welland A, Ely LK, Clements CS, et al. 2010. Constraints within major histocompatibility complex class I restricted peptides: presentation and consequences for T-cell recognition. *PNAS* 107:5534–39
18. Rodgers JR, Cook RG. 2005. MHC class Ib molecules bridge innate and acquired immunity. *Nat. Rev. Immunol.* 5:459–71
19. Girardi E, Zajonc DM. 2012. Molecular basis of lipid antigen presentation by CD1d and recognition by natural killer T cells. *Immunol. Rev.* 250:167–79
20. Davis MM, Bjorkman PJ. 1988. T-cell antigen receptor genes and T-cell recognition. *Nature* 334:395–402
21. Arstila TP, Casrouge A, Baron V, Even J, Kanellopoulos J, Kourilsky P. 1999. A direct estimate of the human αβ T cell receptor diversity. *Science* 286:958–61
22. Garcia KC, Degano M, Pease LR, Huang M, Peterson PA, et al. 1998. Structural basis of plasticity in T cell receptor recognition of a self peptide-MHC antigen. *Science* 279:1166–72
23. Bridgeman JS, Sewell AK, Miles JJ, Price DA, Cole DK. 2012. Structural and biophysical determinants of αβ T-cell antigen recognition. *Immunology* 135:9–18
24. Gras S, Burrows SR, Kjer-Nielsen L, Clements CS, Liu YC, et al. 2009. The shaping of T cell receptor recognition by self-tolerance. *Immunity* 30:193–203

25. Turner SJ, Doherty PC, McCluskey J, Rossjohn J. 2006. Structural determinants of T-cell receptor bias in immunity. *Nat. Rev. Immunol.* 6:883–94
26. Birnbaum ME, Mendoza JL, Sethi DK, Dong S, Glanville J, et al. 2014. Deconstructing the peptide-MHC specificity of T cell recognition. *Cell* 157:1073–87
27. Gras S, Burrows SR, Turner SJ, Sewell AK, McCluskey J, Rossjohn J. 2012. A structural voyage toward an understanding of the MHC-I-restricted immune response: lessons learned and much to be learned. *Immunol. Rev.* 250:61–81
28. Marrack P, Scott-Browne JP, Dai S, Gapin L, Kappler JW. 2008. Evolutionarily conserved amino acids that control TCR-MHC interaction. *Annu. Rev. Immunol.* 26:171–203
29. Kjer-Nielsen L, Clements CS, Purcell AW, Brooks AG, Whisstock JC, et al. 2003. A structural basis for the selection of dominant αβ T cell receptors in antiviral immunity. *Immunity* 18:53–64
30. Stewart-Jones GB, McMichael AJ, Bell JI, Stuart DI, Jones EY. 2003. A structural basis for immunodominant human T cell receptor recognition. *Nat. Immunol.* 4:657–63
31. Gras S, Saulquin X, Reiser J-B, Debeaupuis E, Echasserieau K, et al. 2009. Structural bases for the affinity-driven selection of a public TCR against a dominant human cytomegalovirus epitope. *J. Immunol.* 183:430–37
32. Tynan FE, Burrows SR, Buckle AM, Clements CS, Borg NA, et al. 2005. T cell receptor recognition of a 'super-bulged' major histocompatibility complex class I–bound peptide. *Nat. Immunol.* 6:1114–22
33. Tynan FE, Reid HH, Kjer-Nielsen L, Miles JJ, Wilce MC, et al. 2007. A T cell receptor flattens a bulged antigenic peptide presented by a major histocompatibility complex class I molecule. *Nat. Immunol.* 8:268–76
34. Ladell K, Hashimoto M, Iglesias MC, Wilmann PG, McLaren JE, et al. 2013. A molecular basis for the control of preimmune escape variants by HIV-specific $CD8^+$ T cells. *Immunity* 38:425–36
35. Borg NA, Ely LK, Beddoe T, Macdonald WA, Reid HH, et al. 2005. The CDR3 regions of an immunodominant T cell receptor dictate the 'energetic landscape' of peptide-MHC recognition. *Nat. Immunol.* 6:171–80
36. Kjer-Nielsen L, Clements CS, Brooks AG, Purcell AW, Fontes MR, et al. 2002. The structure of HLA-B8 complexed to an immunodominant viral determinant: peptide-induced conformational changes and a mode of MHC class I dimerization. *J. Immunol.* 169:5153–60
37. Kjer-Nielsen L, Clements CS, Brooks AG, Purcell AW, McCluskey J, Rossjohn J. 2002. The 1.5 Å crystal structure of a highly selected antiviral T cell receptor provides evidence for a structural basis of immunodominance. *Structure* 10:1521–32
38. Ely LK, Beddoe T, Clements CS, Matthews JM, Purcell AW, et al. 2006. Disparate thermodynamics governing T cell receptor–MHC-I interactions implicate extrinsic factors in guiding MHC restriction. *PNAS* 103:6641–46
39. Ishizuka J, Stewart-Jones GB, van der Merwe A, Bell JI, McMichael AJ, Jones EY. 2008. The structural dynamics and energetics of an immunodominant T cell receptor are programmed by its Vβ domain. *Immunity* 28:171–82
40. Motozono C, Kuse N, Sun X, Rizkallah PJ, Fuller A, et al. 2014. Molecular basis of a dominant T cell response to an HIV reverse transcriptase 8-mer epitope presented by the protective allele HLA-B*51:01. *J. Immunol.* 192:3428–34
41. Miles JJ, Bulek AM, Cole DK, Gostick E, Schauenburg AJ, et al. 2010. Genetic and structural basis for selection of a ubiquitous T cell receptor deployed in Epstein-Barr virus infection. *PLoS Pathog.* 6:e1001198
42. Cole DK, Yuan F, Rizkallah PJ, Miles JJ, Gostick E, et al. 2009. Germ line-governed recognition of a cancer epitope by an immunodominant human T-cell receptor. *J. Biol. Chem.* 284:27281–89
43. Archbold JK, Macdonald WA, Gras S, Ely LK, Miles JJ, et al. 2009. Natural micropolymorphism in human leukocyte antigens provides a basis for genetic control of antigen recognition. *J. Exp. Med.* 206:209–19
44. Stewart-Jones GB, Simpson P, van der Merwe PA, Easterbrook P, McMichael AJ, et al. 2012. Structural features underlying T-cell receptor sensitivity to concealed MHC class I micropolymorphisms. *PNAS* 109:E3483–92

45. Luz JG, Huang M, Garcia KC, Rudolph MG, Apostolopoulos V, et al. 2002. Structural comparison of allogeneic and syngeneic T cell receptor–peptide-major histocompatibility complex complexes: a buried alloreactive mutation subtly alters peptide presentation substantially increasing Vβ interactions. *J. Exp. Med.* 195:1175–86
46. Miles JJ, Elhassen D, Borg NA, Silins SL, Tynan FE, et al. 2005. CTL recognition of a bulged viral peptide involves biased TCR selection. *J. Immunol.* 175:3826–34
47. Liu YC, Chen Z, Burrows SR, Purcell AW, McCluskey J, et al. 2012. The energetic basis underpinning T-cell receptor recognition of a super-bulged peptide bound to a major histocompatibility complex class I molecule. *J. Biol. Chem.* 287:12267–76
48. Macdonald WA, Purcell AW, Mifsud NA, Ely LK, Williams DS, et al. 2003. A naturally selected dimorphism within the HLA-B44 supertype alters class I structure, peptide repertoire, and T cell recognition. *J. Exp. Med.* 198:679–91
49. Archbold JK, Macdonald WA, Gras S, Ely LK, Miles JJ, et al. 2009. Natural micropolymorphism in human leukocyte antigens provides a basis for genetic control of antigen recognition. *J. Exp. Med.* 206:209–19
50. Gras S, Chen Z, Miles JJ, Liu YC, Bell MJ, et al. 2010. Allelic polymorphism in the T cell receptor and its impact on immune responses. *J. Exp. Med.* 207:1555–67
51. Liu YC, Chen Z, Neller MA, Miles JJ, Purcell AW, et al. 2014. A molecular basis for the interplay between T cells, viral mutants, and human leukocyte antigen micropolymorphism. *J. Biol. Chem.* 289:16688–98
52. Hoare HL, Sullivan LC, Pietra G, Clements CS, Lee EJ, et al. 2006. Structural basis for a major histocompatibility complex class Ib-restricted T cell response. *Nat. Immunol.* 7:256–64
53. Walpole NG, Kjer-Nielsen L, Kostenko L, McCluskey J, Brooks AG, et al. 2010. The structure and stability of the monomorphic HLA-G are influenced by the nature of the bound peptide. *J. Mol. Biol.* 397:467–80
54. Chen J-L, Stewart-Jones G, Bossi G, Lissin NM, Wooldridge L, et al. 2005. Structural and kinetic basis for heightened immunogenicity of T cell vaccines. *J. Exp. Med.* 201:1243–55
55. Bulek AM, Cole DK, Skowera A, Dolton G, Gras S, et al. 2012. Structural basis for the killing of human beta cells by $CD8^+$ T cells in type 1 diabetes. *Nat. Immunol.* 13:283–89
56. Speir JA, Stevens J, Joly E, Butcher GW, Wilson IA. 2001. Two different, highly exposed, bulged structures for an unusually long peptide bound to rat MHC class I RT1-A^a. *Immunity* 14:81–92
57. Borbulevych OY, Piepenbrink KH, Gloor BE, Scott DR, Sommese RF, et al. 2009. T cell receptor cross-reactivity directed by antigen-dependent tuning of peptide-MHC molecular flexibility. *Immunity* 31:885–96
58. Degano M, Garcia KC, Apostolopoulos V, Rudolph MG, Teyton L, Wilson IA. 2000. A functional hot spot for antigen recognition in a superagonist TCR/MHC complex. *Immunity* 12:251–61
59. Ding Y-H, Baker BM, Garboczi DN, Biddison WE, Wiley DC. 1999. Four A6-TCR/Peptide/HLA-A2 structures that generate very different T cell signals are nearly identical. *Immunity* 11:45–56
60. Baker BM, Gagnon SJ, Biddison WE, Wiley DC. 2000. Conversion of a T cell antagonist into an agonist by repairing a defect in the TCR/peptide/MHC interface: implications for TCR signaling. *Immunity* 13:475–84
61. Luz JG, Huang M, Garcia KC, Rudolph MG, Apostolopoulos V, et al. 2002. Structural comparison of allogenic and syngeneic T cell receptor–peptide-major histocompatibility complex complexes: a buried alloreactive mutation subtly alters peptide presentation substantially increasing Vβ interactions. *J. Exp. Med.* 195:1175–86
62. Reiser JB, Darnault C, Gregoire C, Mosser T, Mazza G, et al. 2003. CDR3 loop flexibility contributes to the degeneracy of TCR recognition. *Nat. Immunol.* 4:241–47
63. Reiser JB, Darnault C, Guimezanes A, Gregoire C, Mosser T, et al. 2000. Crystal structure of a T cell receptor bound to an allogeneic MHC molecule. *Nat. Immunol.* 1:291–97
64. Reiser JB, Gregoire C, Darnault C, Mosser T, Guimezanes A, et al. 2002. A T cell receptor CDR3β loop undergoes conformational changes of unprecedented magnitude upon binding to a peptide/MHC class I complex. *Immunity* 16:345–54

65. Borbulevych OY, Insaidoo FK, Baxter TK, Powell DJ Jr, Johnson LA, et al. 2007. Structures of MART-126/27-35 peptide/HLA-A2 complexes reveal a remarkable disconnect between antigen structural homology and T cell recognition. *J. Mol. Biol.* 372:1123–36
66. Borbulevych OY, Santhanagopolan SM, Hossain M, Baker BM. 2011. TCRs used in cancer gene therapy cross-react with MART-1/Melan-A tumor antigens via distinct mechanisms. *J. Immunol.* 187:2453–63
67. Insaidoo FK, Borbulevych OY, Hossain M, Santhanagopolan SM, Baxter TK, Baker BM. 2011. Loss of T cell antigen recognition arising from changes in peptide and major histocompatibility complex protein flexibility: implications for vaccine design. *J. Biol. Chem.* 286:40163–73
68. Ding YH, Smith KJ, Garboczi DN, Utz U, Biddison WE, Wiley DC. 1998. Two human T cell receptors bind in a similar diagonal mode to the HLA-A2/Tax peptide complex using different TCR amino acids. *Immunity* 8:403–11
69. Gras S, Wilmann PG, Chen Z, Halim H, Liu YC, et al. 2012. A structural basis for varied αβTCR usage against an immunodominant EBV antigen restricted to a HLA-B8 molecule. *J. Immunol.* 188:311–21
70. Liu YC, Miles JJ, Neller MA, Gostick E, Price DA, et al. 2013. Highly divergent T-cell receptor binding modes underlie specific recognition of a bulged viral peptide bound to a human leukocyte antigen class I molecule. *J. Biol. Chem.* 288:15442–54
71. Shimizu A, Kawana-Tachikawa A, Yamagata A, Han C, Zhu D, et al. 2013. Structure of TCR and antigen complexes at an immunodominant CTL epitope in HIV-1 infection. *Sci. Rep.* 3:3097
72. Colf LA, Bankovich AJ, Hanick NA, Bowerman NA, Jones LL, et al. 2007. How a single T cell receptor recognizes both self and foreign MHC. *Cell* 129:135–46
73. Macdonald WA, Chen Z, Gras S, Archbold JK, Tynan FE, et al. 2009. T cell allorecognition via molecular mimicry. *Immunity* 31:897–908
74. Bowerman NA, Colf LA, Garcia KC, Kranz DM. 2009. Different strategies adopted by K^b and L^d to generate T cell specificity directed against their respective bound peptides. *J. Biol. Chem.* 284:32551–61
75. Reinherz EL, Tan K, Tang L, Kern P, Liu J, et al. 1999. The crystal structure of a T cell receptor in complex with peptide and MHC class II. *Science* 286:1913–21
76. Feng D, Bond CJ, Ely LK, Maynard J, Garcia KC. 2007. Structural evidence for a germline-encoded T cell receptor–major histocompatibility complex interaction 'codon.' *Nat. Immunol.* 8:975–83
77. Dai S, Huseby ES, Rubtsova K, Scott-Browne J, Crawford F, et al. 2008. Crossreactive T cells spotlight the germline rules for αβ T cell-receptor interactions with MHC molecules. *Immunity* 28:324–34
78. Garcia KC. 2012. Reconciling views on T cell receptor germline bias for MHC. *Trends Immunol.* 33:429–36
79. Dai S, Crawford F, Marrack P, Kappler JW. 2008. The structure of HLA-DR52c: comparison to other HLA-DRB3 alleles. *PNAS* 105:11893–97
80. Adams JJ, Narayanan S, Liu B, Birnbaum ME, Kruse AC, et al. 2011. T cell receptor signaling is limited by docking geometry to peptide-major histocompatibility complex. *Immunity* 35:681–93
81. Mazza C, Auphan-Anezin N, Gregoire C, Guimezanes A, Kellenberger C, et al. 2007. How much can a T-cell antigen receptor adapt to structurally distinct antigenic peptides? *EMBO J.* 26:1972–83
82. Deng L, Langley RJ, Wang Q, Topalian SL, Mariuzza RA. 2012. Structural insights into the editing of germ-line–encoded interactions between T-cell receptor and MHC class II by Vα CDR3. *PNAS* 109:14960–65
83. Deng L, Langley RJ, Brown PH, Xu G, Teng L, et al. 2007. Structural basis for the recognition of mutant self by a tumor-specific, MHC class II–restricted T cell receptor. *Nat. Immunol.* 8:398–408
84. Miles JJ, Borg NA, Brennan RM, Tynan FE, Kjer-Nielsen L, et al. 2006. TCRα genes direct MHC restriction in the potent human T cell response to a class I-bound viral epitope. *J. Immunol.* 177:6804–14
85. Broughton SE, Petersen J, Theodossis A, Scally SW, Loh KL, et al. 2012. Biased T cell receptor usage directed against human leukocyte antigen DQ8-restricted gliadin peptides is associated with celiac disease. *Immunity* 37:611–21
86. Hahn M, Nicholson MJ, Pyrdol J, Wucherpfennig KW. 2005. Unconventional topology of self peptide–major histocompatibility complex binding by a human autoimmune T cell receptor. *Nat. Immunol.* 6:490–96
87. Harkiolaki M, Holmes SL, Svendsen P, Gregersen JW, Jensen LT, et al. 2009. T cell-mediated autoimmune disease due to low-affinity crossreactivity to common microbial peptides. *Immunity* 30:348–57

88. Hennecke J, Carfi A, Wiley DC. 2000. Structure of a covalently stabilized complex of a human αβ T-cell receptor, influenza HA peptide and MHC class II molecule, HLA-DR1. *EMBO J.* 19:5611–24
89. Maynard J, Petersson K, Wilson DH, Adams EJ, Blondelle SE, et al. 2005. Structure of an autoimmune T cell receptor complexed with class II peptide-MHC: insights into MHC bias and antigen specificity. *Immunity* 22:81–92
90. He XL, Radu C, Sidney J, Sette A, Ward ES, Garcia KC. 2002. Structural snapshot of aberrant antigen presentation linked to autoimmunity: the immunodominant epitope of MBP complexed with I-A^u. *Immunity* 17:83–94
91. Yin Y, Li Y, Kerzic MC, Martin R, Mariuzza RA. 2011. Structure of a TCR with high affinity for self-antigen reveals basis for escape from negative selection. *EMBO J.* 30:1137–48
92. Garcia KC, Radu CG, Ho J, Ober RJ, Ward ES. 2001. Kinetics and thermodynamics of T cell receptor-autoantigen interactions in murine experimental autoimmune encephalomyelitis. *PNAS* 98:6818–23
93. Sewell AK. 2012. Why must T cells be cross-reactive? *Nat. Rev. Immunol.* 12:669–77
94. Sethi DK, Schubert DA, Anders A-K, Heroux A, Bonsor DA, et al. 2011. A highly tilted binding mode by a self-reactive T cell receptor results in altered engagement of peptide and MHC. *J. Exp. Med.* 208:91–102
95. Sethi DK, Gordo S, Schubert DA, Wucherpfennig KW. 2013. Crossreactivity of a human autoimmune TCR is dominated by a single TCR loop. *Nat. Commun.* 4:2623
96. Li Y, Huang Y, Lue J, Quandt JA, Martin R, Mariuzza RA. 2005. Structure of a human autoimmune TCR bound to a myelin basic protein self-peptide and a multiple sclerosis-associated MHC class II molecule. *EMBO J.* 24:2968–79
97. Petersen J, Montserrat V, Mujico JR, Loh KL, Beringer DX, et al. 2014. T-cell receptor recognition of HLA-DQ2-gliadin complexes associated with celiac disease. *Nat. Struct. Mol. Biol.* 21:480–88
98. Clayton G, Kappler J. 2014. Structural basis of chronic beryllium disease: linking allergic hypersensitivity and autoimmunity. *Cell* 158:1–11
99. Illing PT, Vivian JP, Dudek NL, Kostenko L, Chen Z, et al. 2012. Immune self-reactivity triggered by drug-modified HLA-peptide repertoire. *Nature* 486:554–58
100. Stadinski BD, Trenh P, Smith RL, Bautista B, Huseby PG, et al. 2011. A role for differential variable gene pairing in creating T cell receptors specific for unique major histocompatibility ligands. *Immunity* 35:694–704
101. Borg NA, Wun KS, Kjer-Nielsen L, Wilce MC, Pellicci DG, et al. 2007. CD1d-lipid-antigen recognition by the semi-invariant NKT T-cell receptor. *Nature* 448:44–49
102. Wun KS, Borg NA, Kjer-Nielsen L, Beddoe T, Koh R, et al. 2008. A minimal binding footprint on CD1d-glycolipid is a basis for selection of the unique human NKT TCR. *J. Exp. Med.* 205:939–49
103. Scott-Browne JP, Matsuda JL, Mallevaey T, White J, Borg NA, et al. 2007. Germline-encoded recognition of diverse glycolipids by natural killer T cells. *Nat. Immunol.* 8:1105–13
104. Pellicci DG, Patel O, Kjer-Nielsen L, Pang SS, Sullivan LC, et al. 2009. Differential recognition of CD1d-α-galactosyl ceramide by the Vβ8.2 and Vβ7 semi-invariant NKT T cell receptors. *Immunity* 31:47–59
105. Patel O, Pellicci DG, Uldrich AP, Sullivan LC, Bhati M, et al. 2011. $V_\beta 2$ natural killer T cell antigen receptor-mediated recognition of CD1d-glycolipid antigen. *PNAS* 108:19007–12
106. Uldrich AP, Patel O, Cameron G, Pellicci DG, Day EB, et al. 2011. A semi-invariant $V_\alpha 10^+$ T cell antigen receptor defines a population of natural killer T cells with distinct glycolipid antigen–recognition properties. *Nat. Immunol.* 12:616–23
107. Mallevaey T, Clarke AJ, Scott-Browne JP, Young MH, Roisman LC, et al. 2011. A molecular basis for NKT cell recognition of CD1d-self-antigen. *Immunity* 34:315–26
108. López-Sagaseta J, Kung JE, Savage PB, Gumperz J, Adams EJ. 2012. The molecular basis for recognition of CD1d/α-galactosylceramide by a human non-Vα24 T cell receptor. *PLOS Biol.* 10:e1001412
109. Pellicci DG, Clarke AJ, Patel O, Mallevaey T, Beddoe T, et al. 2011. Recognition of β-linked self glycolipids mediated by natural killer T cell antigen receptors. *Nat. Immunol.* 12:827–33
110. Yu ED, Girardi E, Wang J, Zajonc DM. 2011. Cutting edge: structural basis for the recognition of β-linked glycolipid antigens by invariant NKT cells. *J. Immunol.* 187:2079–83

111. López-Sagaseta J, Sibener LV, Kung JE, Gumperz J, Adams EJ. 2012. Lysophospholipid presentation by CD1d and recognition by a human natural killer T-cell receptor. *EMBO J.* 31:2047–59
112. Wun KS, Cameron G, Patel O, Pang SS, Pellicci DG, et al. 2011. A molecular basis for the exquisite CD1d-restricted antigen specificity and functional responses of natural killer T cells. *Immunity* 34:327–39
113. Aspeslagh S, Li Y, Yu ED, Pauwels N, Trappeniers M, et al. 2011. Galactose-modified iNKT cell agonists stabilized by an induced fit of CD1d prevent tumour metastasis. *EMBO J.* 30:2294–305
114. Wun KS, Ross F, Patel O, Besra GS, Porcelli SA, et al. 2012. Human and mouse type I natural killer T cell antigen receptors exhibit different fine specificities for CD1d-antigen complex. *J. Biol. Chem.* 287:39139–48
115. Li Y, Girardi E, Wang J, Yu ED, Painter GF, et al. 2010. The Va14 invariant natural killer T cell TCR forces microbial glycolipids and CD1d into a conserved binding mode. *J. Exp. Med.* 207:2383–93
116. Girardi E, Yu ED, Li Y, Tarumoto N, Pei B, et al. 2011. Unique interplay between sugar and lipid in determining the antigenic potency of bacterial antigens for NKT cells. *PLOS Biol.* 9:e1001189
117. Patel O, Pellicci DG, Gras S, Sandoval-Romero ML, Uldrich AP, et al. 2012. Recognition of CD1d-sulfatide mediated by a type II natural killer T cell antigen receptor. *Nat. Immunol.* 13:857–63
118. Girardi E, Maricic I, Wang J, Mac T-T, Iyer P, et al. 2012. Type II natural killer T cells use features of both innate-like and conventional T cells to recognize sulfatide self antigens. *Nat. Immunol.* 13:851–56
119. Adams EJ, Chien YH, Garcia KC. 2005. Structure of a γδ T cell receptor in complex with the nonclassical MHC T22. *Science* 308:227–31
120. Uldrich AP, Le Nours J, Pellicci DG, Gherardin NA, McPherson KG, et al. 2013. CD1d-lipid antigen recognition by the γδ TCR. *Nat. Immunol.* 14:1137–45
121. Kjer-Nielsen L, Patel O, Corbett AJ, Le Nours J, Meehan B, et al. 2012. MR1 presents microbial vitamin B metabolites to MAIT cells. *Nature* 491:717–23
122. Patel O, Kjer-Nielsen L, Le Nours J, Eckle SB, Birkinshaw R, et al. 2013. Recognition of vitamin B metabolites by mucosal-associated invariant T cells. *Nat. Commun.* 4:2142
123. López-Sagaseta J, Dulberger CL, Crooks JE, Parks CD, Luoma AM, et al. 2013. The molecular basis for Mucosal-Associated Invariant T cell recognition of MR1 proteins. *PNAS* 110:E1771–78
124. López-Sagaseta J, Dulberger CL, McFedries A, Cushman M, Saghatelian A, Adams EJ. 2013. MAIT recognition of a stimulatory bacterial antigen bound to MR1. *J. Immunol.* 191:5268–77
125. Reantragoon R, Corbett AJ, Sakala IG, Gherardin NA, Furness JB, et al. 2013. Antigen-loaded MR1 tetramers define T cell receptor heterogeneity in mucosal-associated invariant T cells. *J. Exp. Med.* 210:2305–20
126. Reantragoon R, Kjer-Nielsen L, Patel O, Chen Z, Illing PT, et al. 2012. Structural insight into MR1-mediated recognition of the mucosal associated invariant T cell receptor. *J. Exp. Med.* 209:761–74
127. Eckle S, Birkinshaw R. 2014. A molecular basis underpinning the T cell receptor heterogeneity of Mucosal-Associated Invariant T cells. *J. Exp. Med.* 211:1585–600
128. Corbett AJ, Eckle SB, Birkinshaw RW, Liu L, Patel O, et al. 2014. T-cell activation by transitory neo-antigens derived from distinct microbial pathways. *Nature* 509:361–65
129. Tikhonova AN, Vann Laethem F, Hanada K-I, Lu J, Pobezinsky LA, et al. 2012. αβ T cell receptors that do not undergo major histocompatibility complex-specific thymic selection possess antibody-like recognition specificities. *Immunity* 36:79–91
130. Yin L, Huseby E, Scott-Browne J, Rubtsova K, Pinilla C, et al. 2011. A single T cell receptor bound to major histocompatibility complex class I and class II glycoproteins reveals switchable TCR conformers. *Immunity* 35:23–33
131. Turner SJ, Kedzierska K, Komodromou H, La Gruta NL, Dunstone MA, et al. 2005. Lack of prominent peptide-major histocompatibility complex features limits repertoire diversity in virus-specific $CD8^+$ T cell populations. *Nat. Immunol.* 6:382–89
132. Day EB, Guillonneau C, Gras S, La Gruta NL, Vignali DAA, et al. 2011. Structural basis for enabling T-cell receptor diversity within biased virus-specific $CD8^+$ T-cell responses. *PNAS* 108:9536–41
133. Auphan-Anezin N, Mazza C, Guimezanes A, Barrett-Wilt GA, Montero-Julian F, et al. 2006. Distinct orientation of the alloreactive monoclonal CD8 T cell activation program by three different peptide/MHC complexes. *Eur. J. Immunol.* 36:1856–66

134. Khan AR, Baker BM, Ghosh P, Biddison WE, Wiley DC. 2000. The structure and stability of an HLA-A*0201/octameric tax peptide complex with an empty conserved peptide-N-terminal binding site. *J. Immunol.* 164:6398–405
135. Scott DR, Borbulevych OY, Piepenbrink KH, Corcelli SA, Baker BM. 2011. Disparate degrees of hypervariable loop flexibility control T-cell receptor cross-reactivity, specificity, and binding mechanism. *J. Mol. Biol.* 414:385–400
136. Zhao R, Loftus DJ, Appella E, Collins EJ. 1999. Structural evidence of T cell xeno-reactivity in the absence of molecular mimicry. *J. Exp. Med.* 189:359–70
137. Buslepp J, Wang H, Biddison WE, Appella E, Collins EJ. 2003. A correlation between TCR Vα docking on MHC and CD8 dependence: implications for T cell selection. *Immunity* 19:595–606
138. Tynan FE, Borg NA, Miles JJ, Beddoe T, El-Hassen D, et al. 2005. High resolution structures of highly bulged viral epitopes bound to major histocompatibility complex class I. Implications for T-cell receptor engagement and T-cell immunodominance. *J. Biol. Chem.* 280:23900–9
139. Maenaka K, Maenaka T, Tomiyama H, Takiguchi M, Stuart DI, Jones EY. 2000. Nonstandard peptide binding revealed by crystal structures of HLA-B*5101 complexed with HIV immunodominant epitopes. *J. Immunol.* 165:3260–67
140. Yin L, Crawford F, Marrack P, Kappler JW, Dai S. 2012. T-cell receptor (TCR) interaction with peptides that mimic nickel offers insight into nickel contact allergy. *PNAS* 109:18517–22
141. Liu X, Dai S, Crawford F, Fruge R, Marrack P, Kappler J. 2002. Alternate interactions define the binding of peptides to the MHC molecule IA^b. *PNAS* 99:8820–25
142. Yoshida K, Corper AL, Herro R, Jabri B, Wilson IA, Teyton L. 2010. The diabetogenic mouse MHC class II molecule $I\text{-}A^{g7}$ is endowed with a switch that modulates TCR affinity. *J. Clin. Investig.* 120:1578–90
143. Newell EW, Ely LK, Kruse AC, Reay PA, Rodriguez SN, et al. 2011. Structural basis of specificity and cross-reactivity in T cell receptors specific for cytochrome c–$I\text{-}E^k$. *J. Immunol.* 186:5823–32
144. Hare BJ, Wyss DF, Osburne MS, Kern PS, Reinherz EL, Wagner G. 1999. Structure, specificity and CDR mobility of a class II restricted single-chain T-cell receptor. *Nat. Struct. Biol.* 6:574–81
145. Zajonc DM, Cantu C 3rd, Mattner J, Zhou D, Savage PB, et al. 2005. Structure and function of a potent agonist for the semi-invariant natural killer T cell receptor. *Nat. Immunol.* 6:810–18
146. Zajonc DM, Savage PB, Bendelac A, Wilson IA, Teyton L. 2008. Crystal structures of mouse CD1d-iGb3 complex and its cognate Vα14 T cell receptor suggest a model for dual recognition of foreign and self glycolipids. *J. Mol. Biol.* 377:1104–16
147. Tyznik AJ, Farber E, Girardi E, Birkholz A, Li Y, et al. 2011. Glycolipids that elicit IFN-γ-biased responses from natural killer T cells. *Chem. Biol.* 18:1620–30
148. Kjer-Nielsen L, Borg NA, Pellicci DG, Beddoe T, Kostenko L, et al. 2006. A structural basis for selection and cross-species reactivity of the semi-invariant NKT cell receptor in CD1d/glycolipid recognition. *J. Exp. Med.* 203:661–73
149. Koch M, Stronge VS, Shepherd D, Gadola SD, Mathew B, et al. 2005. The crystal structure of human CD1d with and without α-galactosylceramide. *Nat. Immunol.* 6:819–26
150. Zajonc DM, Maricic I, Wu D, Halder R, Roy K, et al. 2005. Structural basis for CD1d presentation of a sulfatide derived from myelin and its implications for autoimmunity. *J. Exp. Med.* 202:1517–26